

Geodesics on an ellipsoid of revolution

Charles F. F. Karney*

SRI International, 201 Washington Rd, Princeton, NJ 08543-5300, USA

(Dated: February 7, 2011)

Algorithms for the computation of the forward and inverse geodesic problems for an ellipsoid of revolution are derived. These are accurate to better than 15 nm when applied to the terrestrial ellipsoids. The solutions of other problems involving geodesics (triangulation, projections, maritime boundaries, and polygonal areas) are investigated.

Keywords: geometrical geodesy, geodesics, map projections, triangulation, maritime boundaries, polygonal areas, numerical methods

1. INTRODUCTION

A geodesic is the natural “straight line”, defined as the line of minimum curvature, for the surface of the earth (Hilbert and Cohn-Vossen, 1952, pp. 220–222). Geodesics are also of interest because the shortest path between two points on the earth is always a geodesic (although the converse is not necessarily true). In most terrestrial applications, the earth is taken to be an ellipsoid of revolution and I adopt this model in this paper.

Consider two points A , at latitude and longitude (ϕ_1, λ_1) , and B , at (ϕ_2, λ_2) , on the surface of the earth connected by

a geodesic. Denote the bearings of the geodesic (measured clockwise from north) at A and B by α_1 and α_2 , respectively, and the length of the geodesic by s_{12} ; see Fig. 1. There are two main “geodesic problems”: the *direct* problem, given ϕ_1 , s_{12} , and α_1 determine ϕ_2 , $\lambda_{12} = \lambda_2 - \lambda_1$, and α_2 ; and the *inverse* problem, given the ϕ_1 , ϕ_2 , and λ_{12} , determine s_{12} , α_1 , and α_2 . Considering the ellipsoidal triangle, NAB , in Fig. 1, where N is the north pole, it is clear that both problems are equivalent to solving the triangle given two sides and the included angle. In the first half of this paper (Secs. 2–9), I present solutions to these problems: the accuracy of the solutions is limited only by the precision of the number system of the computer; the direct solution is non-iterative; the inverse solution is iterative but always converges in a few iterations. In the second half (Secs. 10–15), I discuss several applications of geodesics.

This paper has had a rather elephantine gestation. My initial work in this area grew out of a dissatisfaction with the widely used algorithms for the main geodesic problems given by Vincenty (1975a). These have two flaws: firstly, the algorithms are given to a fixed order in the flattening of the ellipsoid thereby limiting their accuracy; more seriously, the algorithm for the inverse problem fails in the case of nearly antipodal points. Starting with the overview of the problem given by Williams (2002), I cured the defects noted above and included the algorithms in GeographicLib (Karney, 2010) in March 2009. At the same time, I started writing this paper and in the course of this I came across references in, for example, Rainsford (1955) to work by Euler, Legendre, and Bessel. Because no specific citations were given, I initially ignored these references. However, when I finally stumbled across Bessel’s paper on geodesics (Bessel, 1825), I was “like some watcher of the skies when a new planet swims into his ken”. Overlooking minor quirks of notation and the use of logarithms for numerical calculations, Bessel gives a formulation and solution of the direct geodesic problem which is as clear, as concise, and as modern as any I have read. However, I was surprised to discover that Bessel derived series expansions for the geodesic integrals which are more economical than those used in the English-language literature of the 20th century. This prompted me to undertake a systematic search for the other

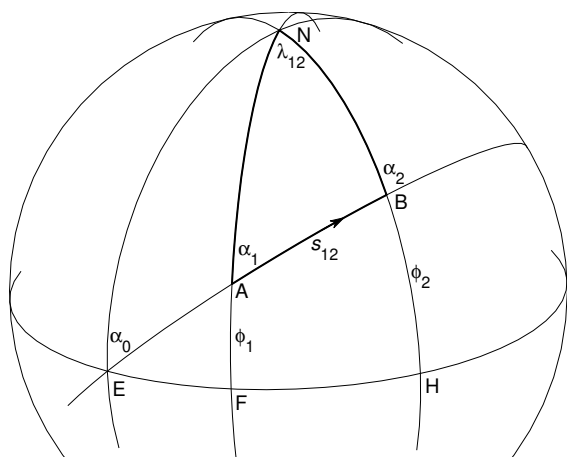


FIG. 1 The ellipsoidal triangle NAB . N is the north pole, NA and NB are meridians, and AB is a geodesic of length s_{12} . The longitude of B relative to A is λ_{12} ; the latitudes of A and B are ϕ_1 and ϕ_2 . EFH is the equator with E also lying on the extension of the geodesic AB ; and α_0 , α_1 , and α_2 are the azimuths of the geodesic at E , A , and B .

*Electronic address: charles.karney@sri.com

original papers on geodesics, the fruits of which are available on-line (Karney, 2009). These contained other little known results—probably the most important of which is the concept of the reduced length (Sect. 3)— which have been incorporated into the geodesic classes in GeographicLib.

Some authors define “spheroid” as an ellipsoid of revolution. In this paper, I use the term in its more general sense, as an approximately spherical figure. Although this paper is principally concerned the earth modeled as an ellipsoid of revolution, there are two sections where the analysis is more general: (1) in the development of the auxiliary sphere, Sect. 2 and Appendix A, which applies to a spheroid of revolution; (2) in the generalization of the gnomonic projection, Sect. 13, which applies to a general spheroid.

2. AUXILIARY SPHERE

The study of geodesics on an ellipsoid of revolution was pursued by many authors in the 18th and 19th centuries. The important early papers are by Clairaut (1735), Euler (1755), Dionis du Séjour (1789, Book 1, Chaps. 1–3), Legendre (1789, 1806), and Oriani (1806, 1808, 1810). Clairaut (1735) found an invariant for a geodesic (a consequence of the rotational symmetry of the ellipsoid); this reduces the equations for the geodesic to quadrature. Subsequently, Legendre (1806) and Oriani (1806) reduced the spheroidal triangle in Fig. 1 into an equivalent triangle on the “auxiliary” sphere. Bessel (1825) provided a method (using tables that he supplied) to compute the necessary integrals and allowed the direct problem to be solved with an accuracy of a few centimeters. In this section, I summarize this formulation of geodesics; more details are given in Appendix A in which the derivation of the auxiliary sphere is given.

I consider an ellipsoid of revolution with equatorial radius a , and polar semi-axis b , flattening f , third flattening n , eccentricity e , and second eccentricity e' given by

$$f = (a - b)/a, \quad (1)$$

$$n = (a - b)/(a + b) = f/(2 - f), \quad (2)$$

$$e^2 = (a^2 - b^2)/a^2 = f(2 - f), \quad (3)$$

$$e'^2 = (a^2 - b^2)/b^2 = e^2/(1 - e^2). \quad (4)$$

In this paper, I am primarily concerned with oblate ellipsoids ($a > b$); however, with a few exceptions, the formulas apply to prolate ellipsoids merely by allowing $f < 0$ and $e^2 < 0$. (Appendix D addresses the modifications necessary to treat prolate ellipsoids in more detail.) Most of the examples in this paper use the WGS84 ellipsoid for which $a = \mathbf{6\,378.137}$ km and $f = \mathbf{1/298.257\,223\,563}$. (In the illustrative examples, numbers given in boldface are exact. The other numbers are obtained by rounding the exact result to the given number of places.) The surface of the ellipsoid is characterized by its meridional and transverse radii of curvature,

$$\rho = \frac{a}{1 - f} w^3, \quad (5)$$

$$\nu = \frac{a}{1 - f} w, \quad (6)$$

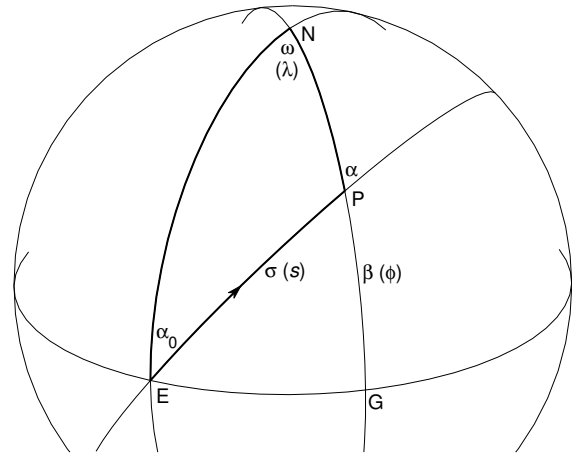


FIG. 2 The elementary ellipsoidal triangle NEP mapped to the auxiliary sphere. NE and NPG are meridians; EG is the equator; and EP is the geodesic. The corresponding ellipsoidal variables are shown in parentheses.

respectively, where

$$w = \frac{1}{\sqrt{1 + e'^2 \cos^2 \phi}}. \quad (7)$$

Consider a geodesic which intersects the equator, $\phi = 0$, in the northwards direction with azimuth (measured clockwise from north) $\alpha_0 \in [-\frac{1}{2}\pi, \frac{1}{2}\pi]$. I denote this equatorial crossing point E and this is taken as the origin for the longitude λ and for measuring (signed) displacements s along the geodesic. Because this definition of longitude depends on the geodesic, longitude differences must be computed for points on the same geodesic. Consider now a point P with latitude ϕ , longitude λ , a displacement s along the geodesic and form the ellipsoidal triangle NEP where N represents the north pole. The (forward) azimuth of the geodesic at P is α (i.e., the angle NPE is $\pi - \alpha$).

Appendix A shows how this triangle may be transferred to the auxiliary sphere where the latitude on the sphere is the *reduced latitude* β , given by

$$\tan \beta = (1 - f) \tan \phi \quad (8)$$

(Legendre, 1806, p. 136), azimuths (α_0 and α) are conserved, the longitude is denoted by ω , and EP is a portion of a great circle with arc length σ ; see Fig. 2. (Cayley (1870, p. 331) suggested the term *parametric latitude* for β because this is the angle most commonly used when the meridian ellipse is written in parametric form.) Applying Napier’s rules of circular parts (Todhunter, 1871, §66) to the right triangle EPG in Fig. 2 gives a set of relations that apply cyclically to $[\alpha_0, \frac{1}{2}\pi - \sigma, \frac{1}{2}\pi - \alpha, \beta, \omega]$,

$$\sin \alpha_0 = \sin \alpha \cos \beta \quad (9)$$

$$= \tan \omega \cot \sigma, \quad (10)$$

$$\cos \sigma = \cos \beta \cos \omega \quad (11)$$

$$= \tan \alpha_0 \cot \alpha, \quad (12)$$

$$\cos \alpha = \cos \omega \cos \alpha_0 \quad (13)$$

$$= \cot \sigma \tan \beta, \quad (14)$$

$$\sin \beta = \cos \alpha_0 \sin \sigma \quad (15)$$

$$= \cot \alpha \tan \omega, \quad (16)$$

$$\sin \omega = \sin \sigma \sin \alpha \quad (17)$$

$$= \tan \beta \tan \alpha_0. \quad (18)$$

In solving the main geodesic problems, I let P stand for A or B with the quantities β , α , σ , ω , s , and λ acquiring a subscript 1 or 2. I also define $\sigma_{12} = \sigma_2 - \sigma_1$, the increase of σ along AB , with ω_{12} , s_{12} , and λ_{12} defined similarly. Equation (9) is Clairaut's characteristic equation for the geodesic, Eq. (A2). The ellipsoidal quantities s and λ are then given by (Bessel, 1825, Eqs. (5))

$$\frac{1}{a} \frac{ds}{d\sigma} = \frac{d\lambda}{d\omega} = w. \quad (19)$$

where w , Eq. (7), is now given in terms of β by

$$w = \sqrt{1 - e^2 \cos^2 \beta}, \quad (20)$$

and where the derivatives are taken holding α_0 fixed (see Appendix A). Integrating the equation for s and substituting for β from Eq. (15) gives (Bessel, 1825, §5)

$$\frac{s}{b} = \int_0^\sigma \sqrt{1 + k^2 \sin^2 \sigma'} d\sigma', \quad (21)$$

where

$$k = e' \cos \alpha_0. \quad (22)$$

As Legendre (1811, §127) points out, the expression for s given by Eq. (21) is the same as that for the length along the perimeter of an ellipse with semi-axes b and $b\sqrt{1+k^2}$. The equation for λ may also be expressed as an integral in σ by using the second of Eqs. (A4), $d\omega/d\sigma = \sin \alpha / \cos \beta$; this gives (Bessel, 1825, §9)

$$\lambda = \omega - f \sin \alpha_0 \int_0^\sigma \frac{2 - f}{1 + (1 - f)\sqrt{1 + k^2 \sin^2 \sigma'}} d\sigma'. \quad (23)$$

Consider a geodesic on the auxiliary sphere completely encircling the sphere. On the ellipsoid, the end point B satisfies $\phi_2 = \phi_1$ and $\alpha_2 = \alpha_1$; however, from Eq. (23), the longitude difference λ_{12} falls short of 2π by approximately $2\pi f \sin \alpha_0$. As a consequence, geodesics on ellipsoids (as distinct from spheres) are not, in general, closed.

In principle, the auxiliary sphere and Eqs. (21) and (23) enable the solution of all geodesic problems on an ellipsoid. However, the efficient solution of the inverse problem requires knowledge of how neighboring geodesics behave. This is examined in the next section.

3. REDUCED LENGTH

Following Bessel's paper, Gauss (1902) studied the properties of geodesics on general surfaces. Consider all the geodesics emanating from a point A . Define a *geodesic circle*

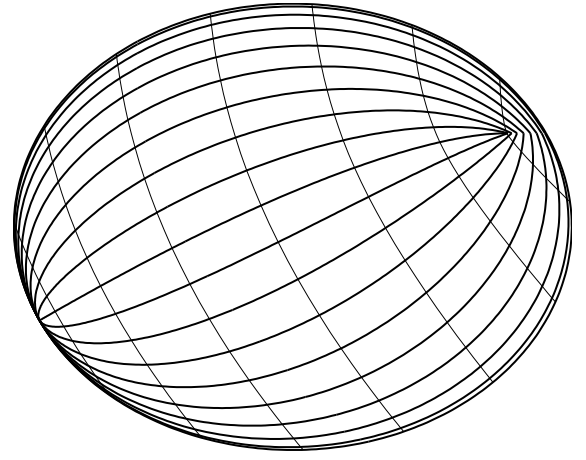


FIG. 3 Geodesics from a point $\phi_1 = -30^\circ$. The east-going geodesics with azimuths α_1 which are multiples of 10° are shown as heavy lines. The spherical arc length of the geodesics is $\sigma_{12} = 180^\circ$. The geodesics are viewed from a distant point over the equator at $\lambda - \lambda_1 = 90^\circ$. The light lines show equally spaced geodesic circles. The flattening of the ellipsoid was taken to be $f = \frac{1}{5}$ for the purposes of this figure.

centered at A to be the locus of points a fixed (geodesic) distance s_{12} from A ; this is a straightforward extension of the definition of a circle on a plane. Gauss (1902, §15) proved that geodesic circles intersect the geodesics at right angles; see Fig. 3.

(Circles on a plane also have a second property: they are the curves which enclose the maximum area for a given perimeter. On an ellipsoid such curves have constant geodesic curvature (Minding, 1830). Darboux (1894, §652) adopts this as his definition of the geodesic circle; however, in general, these curves are different from the geodesic circles as defined in the previous paragraph.)

Gauss (1902) also introduced the concept of the *reduced length* m_{12} for the geodesic which is also the subject of a detailed investigation by Christoffel (1910) (the term is his coinage). Consider two geodesics of length s_{12} departing from A at azimuths α_1 and $\alpha_1 + d\alpha_1$. On a flat surface the end points are separated by $s_{12} d\alpha_1$ (in the limit $d\alpha_1 \rightarrow 0$). On a curved surface the separation is $m_{12} d\alpha_1$ where m_{12} is the reduced length. Gauss (1902, §19) showed that the reduced length satisfies the differential equation

$$\frac{d^2 m}{ds^2} + K(s)m = 0, \quad (24)$$

where $K(s)$ is the Gaussian curvature of the surface. Let $m(s; s_1)$ be the solution to Eq. (24) subject to the initial conditions

$$m(s_1; s_1) = 0, \quad \left. \frac{dm(s; s_1)}{ds} \right|_{s=s_1} = 1;$$

then m_{12} is given by $m_{12} = m(s_2; s_1)$. Equation (24) obeys a simple reciprocity relation $m(s_1; s_2) = -m(s_2; s_1)$ which

gives the result (Christoffel, 1910, §9) that the reduced length is invariant under interchange of the end points, i.e., $m_{21} = -m_{12}$.

For a geodesic on an ellipsoid of revolution, the Gaussian curvature is given by

$$K = \frac{1}{\rho\nu} = \frac{b^2}{a^4 w^4} = \frac{1}{b^2(1+k^2 \sin^2 \sigma)^2}. \quad (25)$$

Helmert (1880, §6.5) solves Eq. (24) in this case to give

$$\begin{aligned} m_{12}/b &= \sqrt{1+k^2 \sin^2 \sigma_2} \cos \sigma_1 \sin \sigma_2 \\ &\quad - \sqrt{1+k^2 \sin^2 \sigma_1} \sin \sigma_1 \cos \sigma_2 \\ &\quad - \cos \sigma_1 \cos \sigma_2 (J(\sigma_2) - J(\sigma_1)), \end{aligned} \quad (26)$$

where

$$\begin{aligned} J(\sigma) &= \int_0^\sigma \frac{k^2 \sin^2 \sigma'}{\sqrt{1+k^2 \sin^2 \sigma'}} d\sigma' \\ &= \frac{s}{b} - \int_0^\sigma \frac{1}{\sqrt{1+k^2 \sin^2 \sigma'}} d\sigma'. \end{aligned} \quad (27)$$

In the spherical limit, Eq. (26) reduces to

$$m_{12} = a \sin \sigma_{12} = a \sin(s_{12}/a).$$

Gauss (1902, §23) also introduced what I call the *geodesic scale* M_{12} , which gives the separation of close, initially parallel, geodesics, and which is given by another solution of Eq. (24), $M(s; s_1)$, with the initial conditions

$$M(s_1; s_1) = 1, \quad \left. \frac{dM(s; s_1)}{ds} \right|_{s=s_1} = 0.$$

Darboux (1894, §633) shows how to construct the solution given two independent solutions of Eq. (24) which are given, for example, by Eq. (26) with two different starting points. This gives

$$\begin{aligned} M_{12} &= \cos \sigma_1 \cos \sigma_2 \\ &\quad + \frac{\sqrt{1+k^2 \sin^2 \sigma_2}}{\sqrt{1+k^2 \sin^2 \sigma_1}} \sin \sigma_1 \sin \sigma_2 \\ &\quad - \frac{\sin \sigma_1 \cos \sigma_2 (J(\sigma_2) - J(\sigma_1))}{\sqrt{1+k^2 \sin^2 \sigma_1}}, \end{aligned} \quad (28)$$

where $M_{12} = M(s_2; s_1)$. Note that M_{12} is *not* symmetric under interchange of the end points. In the spherical limit, Eq. (28) reduces to

$$M_{12} = \cos \sigma_{12} = \cos(s_{12}/a).$$

By direct differentiation, it is easy to show that the Wronskian for the two solutions m_{12} and M_{12} is a constant. Substituting the initial conditions then gives

$$M_{12} \frac{dm_{12}}{ds_2} - m_{12} \frac{dM_{12}}{ds_2} = 1. \quad (29)$$

There is little mention of the reduced length in the geodetic literature in the English language of the last century. An exception is Tobey (1928, Prop. IV) who derives an expression for m_{12} as a series valid for small s_{12}/a (Rapp, 1991, §4.22).

4. PROPERTIES OF THE INTEGRALS

The solution of the main geodesic problems requires the evaluation of the three integrals appearing in Eqs. (21), (27), and (23). In order to approach the evaluation systematically, I write these integrals as

$$I_1(\sigma) = \int_0^\sigma \sqrt{1+k^2 \sin^2 \sigma'} d\sigma', \quad (30)$$

$$I_2(\sigma) = \int_0^\sigma \frac{1}{\sqrt{1+k^2 \sin^2 \sigma'}} d\sigma', \quad (31)$$

$$I_3(\sigma) = \int_0^\sigma \frac{2-f}{1+(1-f)\sqrt{1+k^2 \sin^2 \sigma'}} d\sigma'. \quad (32)$$

In terms of $I_j(\sigma)$, Eqs. (21), (27), and (23) become

$$s/b = I_1(\sigma), \quad (33)$$

$$J(\sigma) = I_1(\sigma) - I_2(\sigma), \quad (34)$$

$$\lambda = \omega - f \sin \alpha_0 I_3(\sigma). \quad (35)$$

The integrals $I_j(\sigma)$ may be expressed in terms of elliptic functions as (Forsyth, 1896; Jacobi, 1855; Luther, 1856)

$$I_1(\sigma) = k'_1 \int_0^{u_1} \text{nd}^2(u', k_1) du', \quad (36)$$

$$I_2(\sigma) = k'_1 u_1, \quad (37)$$

$$\begin{aligned} I_3(\sigma) &= -\frac{(1-f)k'_1}{f \sin^2 \alpha_0} \int_0^{u_1} \frac{\text{nd}^2(u', k_1)}{1 + \cot^2 \alpha_0 \text{cd}^2(u', k_1)} du' \\ &\quad + \frac{\tan^{-1}(\sin \alpha_0 \tan \sigma)}{f \sin \alpha_0}, \end{aligned} \quad (38)$$

where $k_1 = k/\sqrt{1+k^2}$, $k'_1 = \sqrt{1-k_1^2} = 1/\sqrt{1+k^2}$,

$$\text{am}(u_1 - K(k_1), k_1) = \sigma - \frac{1}{2}\pi,$$

$\text{cd}(x, k)$ and $\text{nd}(x, k)$ are Jacobian elliptic functions (Olver *et al.*, 2010, §22.2), $\text{am}(x, k)$ is Jacobi's amplitude function (Olver *et al.*, 2010, §22.16(i)), and $K(k)$ is the complete elliptic integral of the first kind (Olver *et al.*, 2010, §19.2(ii)). The integrals can also be written in closed form as (Legendre, 1811, §§127–128)

$$I_1(\sigma) = \frac{1}{k'_1} E(\sigma - \frac{1}{2}\pi, k_1) - c_1, \quad (39)$$

$$I_2(\sigma) = k'_1 F(\sigma - \frac{1}{2}\pi, k_1) - c_2, \quad (40)$$

$$\begin{aligned} I_3(\sigma) &= -\frac{1-f}{fk'_1 \sin^2 \alpha_0} G(\sigma - \frac{1}{2}\pi, -\cot^2 \alpha_0, k_1) \\ &\quad + \frac{\tan^{-1}(\sin \alpha_0 \tan \sigma)}{f \sin \alpha_0} - c_3, \end{aligned} \quad (41)$$

where

$$\begin{aligned} G(\phi, \alpha^2, k) &= \int_0^\phi \frac{\sqrt{1-k^2 \sin^2 \theta}}{1-\alpha^2 \sin^2 \theta} d\theta \\ &= \left(1 - \frac{k^2}{\alpha^2}\right) \Pi(\phi, \alpha^2, k) + \frac{k^2}{\alpha^2} F(\phi, k), \end{aligned} \quad (42)$$

the integration constants c_j are given by the condition $I_j(0) = 0$, and $F(\phi, k)$, $E(\phi, k)$, and $\Pi(\phi, \alpha^2, k)$ are Legendre's incomplete elliptic integrals of the first, second, and third kinds (Olver *et al.*, 2010, §19.2(ii)).

There are several ways that the integrals may be computed. One possibility is merely to utilize standard algorithms (Bulirsch, 1965; Carlson, 1995) for elliptic functions and integrals for the evaluation of Eqs. (39)–(41). Alternatively, some authors, for example Saito (1970, 1979), have employed numerical quadrature on Eqs. (30) and (32). However, the presence of small parameters in the integrals also allow the integrals to be expressed in terms of rapidly converging series. Bessel (1825) used this approach and tabulated the coefficients appearing in these series thereby allowing the direct geodesic problem to be solved easily and with an accuracy of about 8 decimal digits. I also use this technique because it allows the integrals to be evaluated efficiently and accurately.

Before carrying out the series expansions, it is useful to establish general properties of the integrals. As functions of σ , the integrands are all even, periodic with period π , positive, and of the form $1 + O(f)$. (Note that $k^2 = O(f)$.) The integrals $I_j(\sigma)$ can therefore be expressed as

$$I_j(\sigma) = A_j(\sigma + B_j(\sigma)), \quad \text{for } j = 1, 2, 3, \quad (43)$$

where the constant $A_j = 1 + O(f)$ and $B_j(\sigma) = O(f)$ is odd and periodic with period π and so may be written as

$$B_j(\sigma) = \sum_{l=1}^{\infty} C_{jl} \sin 2l, \sigma \quad \text{for } j = 1, 2, 3. \quad (44)$$

In addition, it is easy to show that $C_{jl} = O(f^l)$. In order to obtain results for s , λ , and m_{12} accurate to order f^L , truncate the sum in Eq. (44) at $l = L$ for $j = 1$ and 2 and at $l = L - 1$ for $j = 3$. (In the equation for λ , Eq. (35), $I_3(\sigma)$ is multiplied by f ; so it is only necessary to compute this integral to order f^{L-1} .) Similarly, the expansions for A_j and C_{jl} may be truncated at order f^L for $j = 1$ and 2 and at order f^{L-1} for $j = 3$.

The form of the trigonometric expansion, Eqs. (43) and (44), and the subsequent expansion of the coefficients as Taylor series in f (or an equivalent small parameter), that I detail in the next section, provide expansions for the integrals which, with a modest number of terms, are valid for arbitrarily long geodesics. This is to be distinguished from a number of approximate methods for short geodesics (Rapp, 1991, §6), which were derived as an aid to computing by hand.

5. SERIES EXPANSIONS OF THE INTEGRALS

Finding explicit expressions for A_j and C_{jl} is simply matter of expanding the integrands for small k and f enabling the integrals to be evaluated. I used the algebra system Maxima (2009) to carry out the necessary expansion, integration, and simplification. Here, I present the expansions to order $L = 8$.

The choice of expansion parameter affects the compactness of the resulting expressions. In the case of I_1 , Bessel intro-

duced a change of variable,

$$k^2 = \frac{4\epsilon}{(1-\epsilon)^2}, \quad (45)$$

$$\epsilon = \frac{\sqrt{1+k^2}-1}{\sqrt{1+k^2}+1} = \frac{k^2}{(\sqrt{1+k^2}+1)^2}, \quad (46)$$

into Eq. (30) to give

$$(1-\epsilon)I_1(\sigma) = \int_0^\sigma \sqrt{1-2\epsilon \cos 2\sigma' + \epsilon^2} d\sigma'. \quad (47)$$

The integrand now exhibits the symmetry that it is invariant under the transformation $\epsilon \rightarrow -\epsilon$ and $\sigma \rightarrow \frac{1}{2}\pi - \sigma$. This results in a series with half the number of terms (compared to a simple expansion in k^2). The relation between k and ϵ is the same as that between the second eccentricity and third flattening of an ellipsoid, e' and n , and frequently formulas for ellipsoids are simpler when expressed in terms of n because of the symmetry of its definition, Eq. (2). (Bessel undertook the task of tabulating the coefficients in the series for $B_1(\sigma)$ for some 200 different values of k . This gave him with a strong incentive to find a way to halve the amount of work required.)

The quantity ϵ is $O(f)$; thus expanding Eq. (47) to order f^8 is, asymptotically, equivalent to expanding to order ϵ^8 . Carrying out this expansion in ϵ then yields

$$\begin{aligned} A_1 &= (1-\epsilon)^{-1} \left(1 + \frac{1}{4}\epsilon^2 + \frac{1}{64}\epsilon^4 + \frac{1}{256}\epsilon^6 \right. \\ &\quad \left. \parallel + \frac{25}{16384}\epsilon^8 + \dots \right), \\ C_{11} &= -\frac{1}{2}\epsilon + \frac{3}{16}\epsilon^3 - \frac{1}{32}\epsilon^5 \parallel + \frac{19}{2048}\epsilon^7 + \dots, \\ C_{12} &= -\frac{1}{16}\epsilon^2 + \frac{1}{32}\epsilon^4 - \frac{9}{2048}\epsilon^6 \parallel + \frac{7}{4096}\epsilon^8 + \dots, \\ C_{13} &= -\frac{1}{48}\epsilon^3 + \frac{3}{256}\epsilon^5 \parallel - \frac{3}{2048}\epsilon^7 + \dots, \\ C_{14} &= -\frac{5}{512}\epsilon^4 + \frac{3}{512}\epsilon^6 \parallel - \frac{11}{16384}\epsilon^8 + \dots, \\ C_{15} &= -\frac{7}{1280}\epsilon^5 \parallel + \frac{7}{2048}\epsilon^7 + \dots, \\ C_{16} &= -\frac{7}{2048}\epsilon^6 \parallel + \frac{9}{4096}\epsilon^8 + \dots, \\ C_{17} &= \parallel - \frac{33}{14336}\epsilon^7 + \dots, \\ C_{18} &= \parallel - \frac{429}{262144}\epsilon^8 + \dots. \end{aligned} \quad (49)$$

I use the caesura symbol, \parallel , to indicate where the series may be truncated, at $O(f^6)$, while still giving full accuracy with double-precision arithmetic for $|f| \leq 1/150$ (this is established in Sect. 9). Equation (49) is a simple extension of series given by Bessel (1825, §5), except that I have divided out the coefficient of the linear term A_1 . Bessel's formulation was used throughout the 19th century and the series given here, truncated to order ϵ^4 , coincides with Helmert (1880, Eq. (5.5.7)). However, many later works, such as Rainsford (1955, Eqs. (18)–(19)), use less efficient expansions in k^2 .

The expansion for I_2 proceeds analogously yielding

$$\begin{aligned} A_2 &= (1-\epsilon) \left(1 + \frac{1}{4}\epsilon^2 + \frac{9}{64}\epsilon^4 + \frac{25}{256}\epsilon^6 \right. \\ &\quad \left. \parallel + \frac{1225}{16384}\epsilon^8 + \dots \right), \\ C_{21} &= \frac{1}{2}\epsilon + \frac{1}{16}\epsilon^3 + \frac{1}{32}\epsilon^5 \parallel + \frac{41}{2048}\epsilon^7 + \dots, \\ C_{22} &= \frac{3}{16}\epsilon^2 + \frac{1}{32}\epsilon^4 + \frac{35}{2048}\epsilon^6 \parallel + \frac{47}{4096}\epsilon^8 + \dots, \end{aligned} \quad (50)$$

$$\begin{aligned}
C_{23} &= \frac{5}{48}\epsilon^3 + \frac{5}{256}\epsilon^5 \parallel + \frac{23}{2048}\epsilon^7 + \dots, \\
C_{24} &= \frac{35}{512}\epsilon^4 + \frac{7}{512}\epsilon^6 \parallel + \frac{133}{16384}\epsilon^8 + \dots, \\
C_{25} &= \frac{63}{1280}\epsilon^5 \parallel + \frac{21}{2048}\epsilon^7 + \dots, \\
C_{26} &= \frac{77}{2048}\epsilon^6 \parallel + \frac{33}{4096}\epsilon^8 + \dots, \\
C_{27} &= \parallel \frac{429}{14336}\epsilon^7 + \dots, \\
C_{28} &= \parallel \frac{6435}{262144}\epsilon^8 + \dots.
\end{aligned} \tag{51}$$

The expansion of I_3 is more difficult because of the presence of two parameters f and k ; this presented a problem for Bessel—it was a practical impossibility for him to compile complete tables of coefficients with two dependencies. Later, when the flattening of the earth was known with some precision, he might have contemplated compiling tables for a few values of f . Instead, Bessel (1825, §8) employs a transformation to move the dependence on the second parameter into a higher order term which he then neglects. The magnitude of the neglected term is about $0.000\,003''$ for geodesics stretching half way around the WGS84 ellipsoid; this corresponds to an error in position of about 0.1 mm. Although this is a very small error, there is no need to resort to such trickery nowadays because computers can evaluate the coefficients as needed.

Following Helmert (1880, Eq. (5.8.14)), I expand in n and ϵ , both of which are $O(f)$, to give

$$\begin{aligned}
A_3 &= 1 - \left(\frac{1}{2} - \frac{1}{2}n\right)\epsilon - \left(\frac{1}{4} + \frac{1}{8}n - \frac{3}{8}n^2\right)\epsilon^2 \\
&\quad - \left(\frac{1}{16} + \frac{3}{16}n + \frac{1}{16}n^2 \parallel - \frac{5}{16}n^3\right)\epsilon^3 \\
&\quad - \left(\frac{3}{64} + \frac{1}{32}n \parallel + \frac{5}{32}n^2 + \frac{5}{128}n^3 + \dots\right)\epsilon^4 \\
&\quad - \left(\frac{3}{128} \parallel + \frac{5}{128}n + \frac{5}{256}n^2 + \dots\right)\epsilon^5 \\
&\quad \parallel - \left(\frac{5}{256} + \frac{15}{1024}n + \dots\right)\epsilon^6 - \frac{25}{2048}\epsilon^7 + \dots,
\end{aligned} \tag{52}$$

$$\begin{aligned}
C_{31} &= \left(\frac{1}{4} - \frac{1}{4}n\right)\epsilon + \left(\frac{1}{8} - \frac{1}{8}n^2\right)\epsilon^2 \\
&\quad + \left(\frac{3}{64} + \frac{3}{64}n - \frac{1}{64}n^2 \parallel - \frac{5}{64}n^3\right)\epsilon^3 \\
&\quad + \left(\frac{5}{128} + \frac{1}{64}n \parallel + \frac{1}{64}n^2 - \frac{1}{64}n^3 + \dots\right)\epsilon^4 \\
&\quad + \left(\frac{3}{128} \parallel + \frac{11}{512}n + \frac{3}{512}n^2 + \dots\right)\epsilon^5 \\
&\quad \parallel + \left(\frac{21}{1024} + \frac{5}{512}n + \dots\right)\epsilon^6 + \frac{243}{16384}\epsilon^7 + \dots, \\
C_{32} &= \left(\frac{1}{16} - \frac{3}{32}n + \frac{1}{32}n^2\right)\epsilon^2 \\
&\quad + \left(\frac{3}{64} - \frac{1}{32}n - \frac{3}{64}n^2 \parallel + \frac{1}{32}n^3\right)\epsilon^3 \\
&\quad + \left(\frac{3}{128} + \frac{1}{128}n \parallel - \frac{9}{256}n^2 - \frac{3}{128}n^3 + \dots\right)\epsilon^4 \\
&\quad + \left(\frac{5}{256} \parallel + \frac{1}{256}n - \frac{1}{128}n^2 + \dots\right)\epsilon^5 \\
&\quad \parallel + \left(\frac{27}{2048} + \frac{69}{8192}n + \dots\right)\epsilon^6 + \frac{187}{16384}\epsilon^7 + \dots, \\
C_{33} &= \left(\frac{5}{192} - \frac{3}{64}n + \frac{5}{192}n^2 \parallel - \frac{1}{192}n^3\right)\epsilon^3 \\
&\quad + \left(\frac{3}{128} - \frac{5}{192}n \parallel - \frac{1}{64}n^2 + \frac{5}{192}n^3 + \dots\right)\epsilon^4 \\
&\quad + \left(\frac{7}{512} \parallel - \frac{1}{384}n - \frac{77}{3072}n^2 + \dots\right)\epsilon^5 \\
&\quad \parallel + \left(\frac{3}{256} - \frac{1}{1024}n + \dots\right)\epsilon^6 + \frac{139}{16384}\epsilon^7 + \dots, \\
C_{34} &= \left(\frac{7}{512} - \frac{7}{256}n \parallel + \frac{5}{256}n^2 - \frac{7}{1024}n^3 + \dots\right)\epsilon^4 \\
&\quad + \left(\frac{7}{512} \parallel - \frac{5}{256}n - \frac{7}{2048}n^2 + \dots\right)\epsilon^5 \\
&\quad \parallel + \left(\frac{9}{1024} - \frac{43}{8192}n + \dots\right)\epsilon^6 + \frac{127}{16384}\epsilon^7 + \dots,
\end{aligned}$$

$$\begin{aligned}
C_{35} &= \left(\frac{21}{2560} \parallel - \frac{9}{512}n + \frac{15}{1024}n^2 + \dots\right)\epsilon^5 \\
&\quad \parallel + \left(\frac{9}{1024} - \frac{15}{1024}n + \dots\right)\epsilon^6 + \frac{99}{16384}\epsilon^7 + \dots, \\
C_{36} &= \parallel \left(\frac{11}{2048} - \frac{99}{8192}n + \dots\right)\epsilon^6 + \frac{99}{16384}\epsilon^7 + \dots, \\
C_{37} &= \parallel \frac{429}{114688}\epsilon^7 + \dots.
\end{aligned} \tag{53}$$

I continue these expansions out to order f^7 , which is, as noted as the end of Sect. 4, consistent with expanding the other integrals to order f^8 . All the parenthetical terms in Eqs. (52) and (53) are functions of n only and so may be evaluated once for a given ellipsoid. Note that the coefficient of ϵ^l is a *terminating* polynomial of order l in n . This is a curious degeneracy of this integral when expressed in terms of n and ϵ . Rainsford (1955, Eqs. (10)–(11)) writes k^2 in Eq. (23) in terms of f and $\cos^2 \alpha_0$ and gives a expansion for the integral in powers of f . This results in an expansion with more terms.

The direct geodesic problem requires solving Eq. (21) for σ in terms of s . (There is a unique solution because $ds/d\sigma > 0$.) Equations (33) and (43), with $j = 1$, can be written as

$$\tau = \sigma + B_1(\sigma), \tag{54}$$

where

$$\tau = s/(bA_1), \tag{55}$$

which shows that finding σ as a function of s is equivalent to inverting Eq. (54). This may be accomplished using Lagrange (1869, §16) inversion, which gives

$$\sigma = \tau + B'_1(\tau), \tag{56}$$

where

$$B'_j(\tau) = \sum_{l=1}^{\infty} \frac{(-1)^l}{l!} \frac{d^{l-1}B_j(\sigma)^l}{d\sigma^{l-1}} \Big|_{\sigma=\tau}.$$

Carrying out these operations with Maxima (2009) gives

$$B'_j(\tau) = \sum_{l=1}^{\infty} C'_{jl} \sin 2l\tau, \tag{57}$$

where

$$\begin{aligned}
C'_{11} &= \frac{1}{2}\epsilon - \frac{9}{32}\epsilon^3 + \frac{205}{1536}\epsilon^5 \parallel - \frac{4879}{73728}\epsilon^7 + \dots, \\
C'_{12} &= \frac{5}{16}\epsilon^2 - \frac{37}{96}\epsilon^4 + \frac{1335}{4096}\epsilon^6 \parallel - \frac{86171}{368640}\epsilon^8 + \dots, \\
C'_{13} &= \frac{29}{96}\epsilon^3 - \frac{75}{128}\epsilon^5 \parallel + \frac{2901}{4096}\epsilon^7 + \dots, \\
C'_{14} &= \frac{539}{1536}\epsilon^4 - \frac{2391}{2560}\epsilon^6 \parallel + \frac{1082857}{737280}\epsilon^8 + \dots, \\
C'_{15} &= \frac{3467}{7680}\epsilon^5 \parallel - \frac{28223}{18432}\epsilon^7 + \dots, \\
C'_{16} &= \frac{38081}{61440}\epsilon^6 \parallel - \frac{733437}{286720}\epsilon^8 + \dots, \\
C'_{17} &= \parallel \frac{459485}{516096}\epsilon^7 + \dots, \\
C'_{18} &= \parallel \frac{109167851}{82575360}\epsilon^8 + \dots.
\end{aligned} \tag{58}$$

Legendre (1806, §13) makes a half-hearted attempt at inverting Eq. (21) in terms of trigonometric functions of s/b (instead of $s/(bA_1)$). Because the period is slightly different from π , the result is a much more messy expansion than

given here. Oriani (1833) used Lagrange inversion to solve the distance integral as a series in k^2 . Finally, Helmert (1880, Eq. (5.6.8)) carries out the inversion in terms of ϵ (as here) including terms to order ϵ^3 .

Most other authors invert Eq. (21) iteratively. Both Bessel (1825) and Vincenty (1975a) use the scheme given by the first line of

$$\begin{aligned}\sigma^{(i+1)} &= \tau - B_1(\sigma^{(i)}) \\ &= \sigma^{(i)} + \frac{s/b - I_1(\sigma^{(i)})}{A_1},\end{aligned}$$

with $\sigma^{(0)} = \tau$. This converges linearly and this is adequate to achieve accuracies on the order of 0.1 mm. A superior iterative solution is given by Newton's method which can be written as

$$\sigma^{(i+1)} = \sigma^{(i)} + \frac{s/b - I_1(\sigma^{(i)})}{\sqrt{1 + k^2 \sin^2 \sigma^{(i)}}},$$

which converges quadratically enabling the solution to full machine precision to be found in a few iterations. The simple iterative scheme effectively replaces the denominator in the fraction above by its mean value A_1 . By using the reverted series, I solve for σ non-iteratively. This does incur the cost of evaluating the coefficients C'_{1l} ; however, this cost can be amortized if several points along the same geodesics are computed.

I give the expansions for A_j , C_{jl} , and C'_{1l} to order f^8 above. However, these expansions are generated by Maxima (2009) with only a few dozen lines of code in about 4 seconds. The expansions can easily be extended to higher order just by changing one parameter in the Maxima code; this has been tested by generating the series to order f^{30} , which takes about 13 minutes. Maxima is also used to generate the C++ code for the expansions in GeographicLib. Treating Maxima as a preprocessor for the C++ compiler, the methods presented here can be considered to be of arbitrary order. In the current GeographicLib implementation, the order of the expansion is a compile-time constant which can be set to any $L \leq 8$. As a practical matter, the series truncated at order f^6 suffice to give close to full accuracy with double-precision arithmetic for terrestrial ellipsoids.

Although Oriani (1806) and Bessel (1825) give expressions for general terms in their expansions, most subsequent authors are content to work out just a few terms. An exception is the work of Levallois and Dupuy (1952) who formulate the problem in terms of Wallis integrals where the general term in the series is given by a recursion relation, allowing the series to be extended to arbitrary order at run-time (Levallois, 1970, Chap. 5). Pittman (1986) independently derived a similar method. Unfortunately, Pittman uses β as the variable of integration (instead of σ); because the latitude does not change monotonically along the geodesic, this choice leads to a loss of numerical accuracy and to technical problems in following geodesics through vertices (the positions of extrema of the latitude for the geodesic).

Because of their widespread adoption, the expansions given by Vincenty (1975a) are of special interest. He expresses

the distance integral in terms of C_{11} and the longitude integral in terms of $1 - A_3$. This leads to rather compact series when truncated at order f^3 . However, much of the simplicity disappears at the next higher order, at which point Vincenty's technique offers no particular advantage. Nevertheless, his procedure does expose the symmetry between k and σ in $I_1(\sigma)$ even though his original expansion was in k^2 . Belatedly, Vincenty (1975a, addendum) discovered the economy of Bessel's change of variable, Eq. (45), to obtain the same expansions for A_1 and C_{11} as given here (truncated at order ϵ^3). Incidentally, the key constraint that Vincenty worked under was that his programs should fit onto calculators, such as the Wang 720 (Vincenty, 1975b, p. 10), which only had a few kilobytes of memory; this precluded the use of higher-order expansions and allowed for only a simple (and failure prone) iterative solution of the inverse problem. Vincenty cast the series in "nested", i.e., Horner, form, in order to minimize program size and register use; I also use the Horner scheme for evaluating the series because of its accuracy and speed.

6. DIRECT PROBLEM

The direct geodesic problem is to determine ϕ_2 , λ_{12} , and α_2 , given ϕ_1 , α_1 and s_{12} ; see Fig. 1. The solution starts by finding β_1 using Eq. (8); next solve the spherical triangle NEA , to give α_0 , σ_1 , and ω_1 , by means of Eqs. (9), (14), and (10). With α_0 known, the coefficients A_j , C_{jl} , and C'_{1l} may be computed from the series in Sect. 5. These polynomials are most easily computed using the Horner scheme and the Maxima program accompanying GeographicLib creates the necessary code. The functions $B_j(\sigma)$ and $B'_1(\sigma)$, Eqs. (44) and (57), may similarly be evaluated for a given σ using Clenshaw (1955) summation, wherein the truncated series,

$$f(x) = \sum_{l=1}^L a_l \sin lx,$$

is computed by determining

$$b_l = \begin{cases} 0, & \text{for } l > L, \\ a_l + 2b_{l+1} \cos x - b_{l+2}, & \text{otherwise,} \end{cases} \quad (59)$$

and by evaluating the sum as

$$f(x) = b_1 \sin x.$$

Now s_1 and λ_1 can be determined using Eqs. (33), (35), and (43). Compute $s_2 = s_1 + s_{12}$ and find σ_2 using Eqs. (55) and (56). Solve the spherical triangle NEB to give β_2 , α_2 , and ω_2 using Eqs. (15), (12), and (10). Find ϕ_2 using Eq. (8) again. With σ_2 and ω_2 given, λ_2 can be found from Eq. (35) which yields $\lambda_{12} = \lambda_2 - \lambda_1$.

Although the reduced length m_{12} is not needed to solve the direct problem, it is nonetheless a useful quantity to compute. It is found using Eqs. (26), (34), (43), (44), (50), and (51). In forming $I_1(\sigma) - I_2(\sigma)$ in Eq. (34), I avoid the loss of precision in the term proportional to σ by writing

$$A_1\sigma - A_2\sigma = (A_1 - 1)\sigma - (A_2 - 1)\sigma,$$

where $A_1 - 1$, for example, is given, from Eq. (48), by

$$A_1 - 1 = (1 - \epsilon)^{-1} \left(\epsilon + \frac{1}{4}\epsilon^2 + \frac{1}{64}\epsilon^4 + \dots \right).$$

The geodesic scales M_{12} and M_{21} may be found similarly, starting with Eq. (28). This completes the solution of the direct geodesic problem.

If several points are required along a single geodesic, many of the intermediate expressions above may be evaluated just once; this includes all the quantities with a subscript “1”, and the coefficients A_j, C_{jl}, C'_{1l} . In this case the determination of the points entails just two Clenshaw summations and a little spherical trigonometry. If it is only necessary to obtain points which are *approximately* evenly spaced on the geodesic, replace s_{12} in the specification of the direct problem with the arc length on the auxiliary sphere σ_{12} , in which case the conversion from τ to σ is avoided and only one Clenshaw summation is needed.

For speed and accuracy, I avoid unnecessarily invoking trigonometric and inverse trigonometric functions. Thus I usually represent an angle θ by the pair the pair $(\sin \theta, \cos \theta)$; however, I avoid the loss of accuracy that may ensue when computing $\cos \alpha_0$, for example, using $\sqrt{1 - \sin^2 \alpha_0}$. Instead, after finding the sine of α_0 using Eq. (9), I compute its cosine with

$$\cos \alpha_0 = \sqrt{\cos^2 \alpha + \sin^2 \alpha \sin^2 \beta};$$

similarly, after finding $\sin \beta$ with Eq. (15), I use

$$\cos \beta = \sqrt{\sin^2 \alpha_0 + \cos^2 \alpha_0 \cos^2 \sigma}.$$

In this way, the angles near the 4 cardinal directions can be represented accurately. In order to determine the quadrant of angles correctly, I replace Eqs. (10), (12), and (14) by

$$\omega = \text{ph}(\cos \sigma + i \sin \alpha_0 \sin \sigma), \quad (60)$$

$$\alpha = \text{ph}(\cos \sigma \cos \alpha_0 + i \sin \alpha_0), \quad (61)$$

$$\sigma = \text{ph}(\cos \alpha \cos \beta + i \sin \beta), \quad (62)$$

where $\theta = \text{ph}(x + iy)$ is the phase of a complex number (Olver *et al.*, 2010, §1.9(i)), typically given by the library function $\text{atan2}(y, x)$. Equations (60) and (61) become indeterminate at the poles, where $\sin \alpha_0 = \cos \sigma = 0$. However, I ensure that ω (and hence λ) and α are consistent with their interpretation for a latitude very close to the pole (i.e., $\cos \beta$ is a small positive quantity) and that the direction of the geodesic in three-dimensional space is correct. In some contexts, the solution requires explicit use of the arc length σ instead of its sine or cosine, for example, in the term $A_j \sigma$ in Eq. (43) and in determining σ from Eq. (56).

Geodesics which encircle the earth multiple times can be handled by allowing s_{12} and σ_{12} to be arbitrarily large. Furthermore, Eq. (60) allows ω to be followed around the circle in synchronism with σ ; this permits the longitude to be tracked continuously along the geodesic so that it increases by $+360^\circ$ (resp. -360°) with each circumnavigation of the earth in the easterly (resp. westerly) direction.

The solution for the direct geodesic problem presented here is a straightforward extension to higher order of Helmert’s method (Helmert, 1880, §5.9), which is largely based on Bessel (1825). These authors, in common with many more recent ones, express the difference of the trigonometric terms which arise when the sums, Eq. (44), in $B_j(\sigma_2) - B_j(\sigma_1)$ are expanded as

$$\sin 2l\sigma_2 - \sin 2l\sigma_1 = 2 \cos(l(\sigma_2 + \sigma_1)) \sin l\sigma_{12}.$$

This substitution is needed to prevent errors in the evaluation of the terms on the left side of the equation causing large relative errors in the difference when using low-precision arithmetic. However, the use of double-precision arithmetic renders this precaution unnecessary (see Sect. 9); furthermore its use interferes with Clenshaw summation and prevents the efficient evaluation of many points along a geodesic.

7. BEHAVIOR NEAR THE ANTIPODAL POINT

Despite the seeming equivalence of the direct and inverse geodesic problems when considered as exercises in ellipsoidal trigonometry, the inverse problem is significantly more complex when transferred to the auxiliary sphere. The included angle for the inverse problem on the ellipsoid is λ_{12} ; however, the equivalent angle ω_{12} on the sphere cannot be immediately determined because the relation between λ and ω , Eq. (23), depends on the unknown angle α_0 . The normal approach, epitomized by Rainsford (1955) and Vincenty (1975a), is to estimate α_1 and α_2 , for example, by approximating the ellipsoid by a sphere (i.e., $\omega_{12} = \lambda_{12}$), obtain a corrected ω_{12} from Eq. (23) and to iterate until convergence. This procedure breaks down if α_1 and α_2 depend very sensitively on ω_{12} , i.e., for nearly antipodal points. Before tackling the inverse problem, it is therefore useful to examine the behavior of geodesics in this case.

Consider two geodesics starting at A with azimuths α_1 and $\alpha_1 + d\alpha_1$. On a closed surface, they will intersect at some distance from A . The first such intersection is the *conjugate point* for the geodesic and it satisfies $m_{12} = 0$ (for $s_{12} > 0$). Jacobi (1891) showed that the geodesics no longer retain the property of being the shortest path beyond the conjugate point (Darboux, 1894, §623). For an ellipsoid with small flattening, the conjugate point is given by

$$\begin{aligned} \phi_2 &= -\phi_1 - f\pi \cos^2 \phi_1 \cos^3 \alpha_1 + O(f^2), \\ \lambda_2 &= \lambda_1 + \pi - f\pi \cos \phi_1 \sin^3 \alpha_1 + O(f^2). \end{aligned}$$

The envelope of the geodesics leaving A is given by the locus of the conjugate points and, in the case of an ellipsoid, this yields a four-point star called an *astroïd* (Jacobi, 1891, Eqs. (16)–(17)), whose equation in cartesian form is, after suitable scaling (see below),

$$x^{2/3} + y^{2/3} = 1, \quad (63)$$

which is depicted in Fig. 4a; see also Jacobi (1891, Fig. 11) and Helmert (1880, §7.2). The angular extent of the astroïd is,

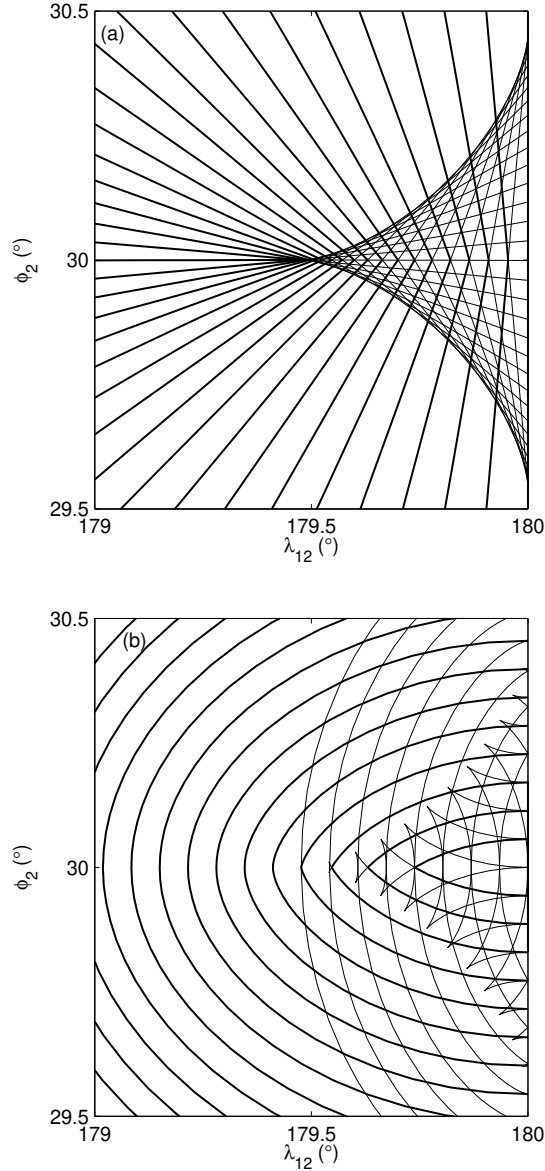


FIG. 4 Geodesics in antipodal region. (a) The geodesics emanating from a point $\phi_1 = -30^\circ$ are shown close in the neighborhood of the antipodal point at $\phi_2 = 30^\circ$, $\lambda_{12} = 180^\circ$. The azimuths α_1 are multiples of 5° between 0° and 180° . The geodesics are given in an equidistant cylindrical projection with the scale set for $\phi_2 = 30^\circ$. The heavy lines are geodesics which satisfy the shortest distance property; the light lines are their continuation. The WGS84 ellipsoid is used. (b) The geodesic circles on the same scale. The heavy (resp. light) lines are for geodesics which have (resp. do not have) are property of being shortest paths. The cusps on the circles lie on the geodesic envelope in (a).

to lowest order, $2f\pi \cos^2 \phi_1$. Figure 4b shows the behavior of the geodesic circles in this region.

Although geodesics are no longer the shortest paths beyond the conjugate point (where they intersect a nearby geodesic), in general, they lose this property earlier when they first intersect any geodesic of the same length emanating from the

same starting point. In the case of the ellipsoid, it is easy to establish earlier intersection points. Consider two geodesics leaving A with azimuths α_1 and $\pi - \alpha_1$. These intersect at $|\omega_{12}| = \pi$ and $\phi_2 = -\phi_1$ and, for oblate ellipsoids this intersection is earlier than the conjugate points. For prolate ellipsoids the corresponding pair of azimuths are $\pm\alpha_1$ and these intersect at $|\lambda_{12}| = \pi$, also prior to the conjugate points. Thus, an ellipsoidal geodesic is the shortest path if, and only if,

$$\max(|\omega_{12}|, |\lambda_{12}|) \leq \pi.$$

The only conjugate points lying on shortest paths are for the geodesics with $\alpha_1 = \pm\frac{1}{2}\pi$ for oblate ellipsoids and $\alpha_1 = 0$ or π for prolate ellipsoids. Solving the inverse problem with end points close to such conjugate pairs presents a challenge because tiny changes in end points lead to large changes in the geodesic.

The inverse problem may be solved approximately in the case of nearly antipodal points by considering the point B together with envelope of geodesics for A (centered at the antipodes of A); see Fig. 5. The coordinates near the antipodes can be rescaled as

$$x = \frac{\sin(\lambda - \lambda_1 - \pi)}{\Delta\lambda}, \quad y = \frac{\sin(\beta + \beta_1)}{\Delta\beta},$$

where

$$\Delta\lambda = f\pi A_3 \cos \beta_1, \quad \Delta\beta = \cos \beta_1 \Delta\lambda,$$

and A_3 is evaluated with $\alpha_0 = \frac{1}{2}\pi - |\beta_1|$. In the (x, y) coordinate system, the conjugate point for the geodesic leaving A with $\alpha_1 = \pm\frac{1}{2}\pi$ is at $(\mp 1, 0)$ and the scale in the y direction compared to x is $1 + O(f)$. The geodesic through B is tangent to the astroid; plane geometry can therefore be used to find its direction, using

$$\frac{x}{\cos \theta} - \frac{y}{\sin \theta} + 1 = 0, \quad (64)$$

where $\theta = \frac{1}{2}\pi - \alpha_2 \approx \alpha_1 - \frac{1}{2}\pi$ is the angle of the geodesic measured anticlockwise from the x axis. The constant term on the left hand side of Eq. (64), 1, reflects the property of tangents to the astroid, that the length CD is constant. (The astroid is the envelope generated as a ladder slides down a wall.) Note that geodesics are directed lines; thus a distinct line is given by $\theta \rightarrow \theta + \pi$. The point of tangency of Eq. (64) with the astroid is

$$x_0 = -\cos^3 \theta, \quad y_0 = \sin^3 \theta,$$

which are the parametric equations for the astroid, Eq. (63); the line and the astroid are shown in Fig. 5a. The goal now is, given x and y (the position of B), to solve Eq. (64) for θ . I follow the method given by Vermeille (2002) for converting from geocentric to geodetic coordinates. In Fig. 5b, COD and BED are similar triangles; if the (signed) length BC is κ , then an equation for κ can be found by applying Pythagoras' theorem to COD ,

$$\frac{x^2}{(1 + \kappa)^2} + \frac{y^2}{\kappa^2} = 1,$$

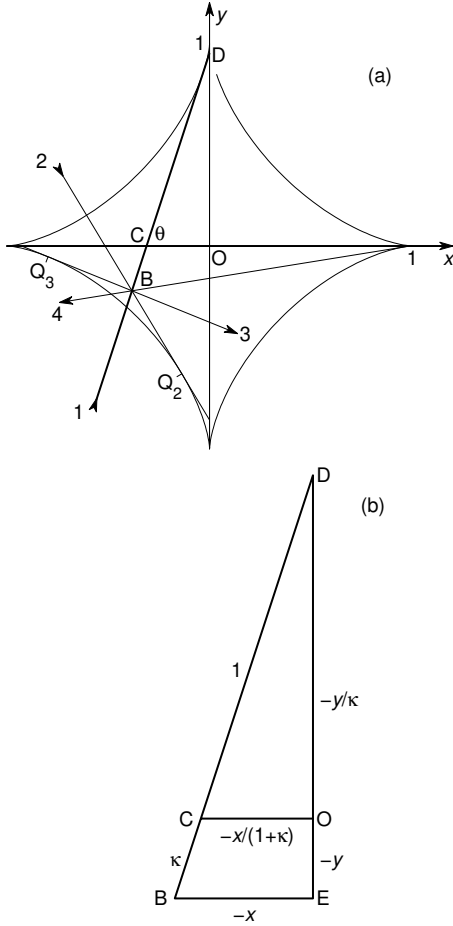


FIG. 5 The inverse geodesic problem for nearly antipodal points. (a) The heavy line (labeled 1) shows the shortest geodesic from A to B continued until it intersects the antipodal meridian at D . The light lines (2–4) show 3 other approximately hemispherical geodesics. The geodesics are all tangent (at their points of conjugacy) to the astroid in this figure. The points Q_2 and Q_3 are the points of conjugacy for the geodesics 2 and 3. (b) The solution of the astroid equations by similar triangles.

which can be expanded to give a quartic equation in κ ,

$$\kappa^4 + 2\kappa^3 + (1 - x^2 - y^2)\kappa^2 - 2y^2\kappa - y^2 = 0. \quad (65)$$

Once κ is known, θ can be determined from the triangle COD in Fig. 5b,

$$\theta = \text{ph}\left(-x/(1 + \kappa) - iy/\kappa\right). \quad (66)$$

The point C in Fig. 5 corresponds to a spherical longitude difference of π . Thus the spherical longitude difference for B , ω_{12} , can be estimated as

$$\omega_{12} \approx \pi + \frac{\kappa x}{1 + \kappa} \Delta\lambda; \quad (67)$$

compare with Helmert (1880, Eq. (7.3.11)).

In Appendix B, I summarize the closed form solution of Eq. (65) as given by Vermeille (2002). I have modified this

TABLE 1 The four approximately hemispherical solutions of the inverse geodesic problem on the WGS84 ellipsoid for $\phi_1 = -30^\circ$, $\phi_2 = 29.9^\circ$, $\lambda_{12} = 179.8^\circ$, ranked by length s_{12} .

No.	α_1 ($^\circ$)	α_2 ($^\circ$)	s_{12} (m)	σ_{12} ($^\circ$)	m_{12} (m)
1	161.891	18.091	19 989 833	179.895	57 277
2	30.945	149.089	20 010 185	180.116	24 241
3	68.152	111.990	20 011 887	180.267	-22 649
4	-81.076	-99.282	20 049 364	180.631	-68 796

solution so that it is applicable for all x and y and more stable numerically.

Equation (65) has 2 (resp. 4) real roots if B lies outside (resp. inside) the astroid. The methods given in Appendix B (with e set to unity) can be used to determine all these roots, κ , and Eq. (66) then gives the corresponding angles of the geodesics at B . All the geodesics obtained in this way are approximately hemispherical and that obtained using the largest value of κ is the shortest path. If B lies on the axes within the astroid, then the limiting solutions Eqs. (B6) or (B7) should be used to avoid an indeterminate expression. For example, if $y = 0$, substitute the largest κ from Eq. (B7) into Eq. (66) to give $\theta = \text{ph}(-x + i\sqrt{\max(0, 1 - x^2)})$.

Figure 5 shows a case where B is within the astroid resulting in 4 hemispherical geodesics which are listed in Table 1 ranked by their length. The values given here have been accurately computed for the case of the WGS84 ellipsoid using the method described in Sect. 8. The second and third geodesics are eastward (the same sense as the shortest geodesic), while the last is westward. As B crosses the boundary of the astroid the second and third geodesics approach one another and disappear (leaving the first and fourth geodesics). Figure 5a also illustrates that the envelope is an evolute of the geodesics; in particular, Eisenhart (1909, §94) shows that the length of geodesic 2 from A to its conjugate point Q_2 exceeds the length of geodesic 3 from A to Q_3 by the distance along the envelope from Q_3 to Q_2 ; see also Helmert (1880, §9.2).

Schmidt (2000) uses Helmert's method for estimating the azimuth. Bowring (1996) proposed a solution of the astroid problem where he approximates the 4 arcs of the astroid by quarter circles. Rapp (1993, Table 1.6, p. 54) gives a similar set of hemispherical geodesics to those given in Table 1. However, this table contains two misprints: ϕ_2 should be $-40^\circ 01' 05.759 32''$ and not $-40^\circ 00' 05.759 32''$; for method 3, α_{12} should be $86^\circ 20' 38.153 06''$ and not $87^\circ 20' 38.153 06''$.

8. INVERSE PROBLEM

Recall that the inverse geodesic problem is to determine s_{12} , α_1 and α_2 given ϕ_1 , ϕ_2 , and λ_{12} . I begin by reviewing the solution of the inverse problem assuming that ω_{12} is given (which is equivalent to seeking the solution of the inverse problem for a sphere). Write the cartesian coordinates for the two end points on the auxiliary sphere (with unit ra-

dius) as $\mathbf{A} = [\cos \beta_1, 0, \sin \beta_1]$ and $\mathbf{B} = [\cos \beta_2 \cos \omega_{12}, \cos \beta_2 \sin \omega_{12}, \sin \beta_2]$. A point on the geodesic a small spherical arc length $d\sigma$ from A is at position $\mathbf{A} + d\mathbf{A}$ where $d\mathbf{A} = [-\sin \beta_1 \cos \alpha_1, \sin \alpha_1, \cos \beta_1 \cos \alpha_1] d\sigma$. The azimuth α_1 can be found by demanding that \mathbf{A} , \mathbf{B} , and $d\mathbf{A}$ be coplanar or that $\mathbf{A} \times \mathbf{B}$ and $\mathbf{A} \times d\mathbf{A}$ be parallel (where \times here denotes the vector cross product), and similarly for α_2 . Likewise, the spherical arc length σ_{12} is given by $\text{ph}(\mathbf{A} \cdot \mathbf{B} + i |\mathbf{A} \times \mathbf{B}|)$, where \cdot denotes the vector dot product. Evaluating these expressions gives

$$\begin{aligned} z_1 &= \cos \beta_1 \sin \beta_2 - \sin \beta_1 \cos \beta_2 \cos \omega_{12} \\ &\quad + i \cos \beta_2 \sin \omega_{12}, \\ z_2 &= -\sin \beta_1 \cos \beta_2 + \cos \beta_1 \sin \beta_2 \cos \omega_{12} \\ &\quad + i \cos \beta_1 \sin \omega_{12}, \\ \alpha_1 &= \text{ph } z_1, \end{aligned} \quad (68)$$

$$\alpha_2 = \text{ph } z_2, \quad (69)$$

$$\sigma_{12} = \text{ph}(\sin \beta_1 \sin \beta_2 + \cos \beta_1 \cos \beta_2 \cos \omega_{12} + i |z_1|). \quad (70)$$

In order to maintain accuracy when A and B are nearly coincident or nearly antipodal, I evaluate the real part of z_1 as

$$\sin(\beta_2 \mp \beta_1) \pm \frac{\sin^2 \omega_{12} \sin \beta_1 \cos \beta_2}{1 \pm \cos \omega_{12}},$$

where the upper and lower signs are for $\cos \omega_{12} \gtrless 0$. The evaluation of z_2 is handled in the same way. This completes the solution of the inverse problem for a sphere.

In the ellipsoidal case, the inverse problem is just a two-dimensional root finding problem. Solve the direct geodesic starting at A and adjust α_1 and s_{12} (subject to the shortest distance constraint), so that the terminal point of the geodesic matches B . In order to convert this process into an algorithm, a rule needs to be given for adjusting α_1 and σ_{12} so that the process converges to the true solution.

The first step in finding such a rule is to convert the two-dimensional problem into a one-dimensional root-finding one. I begin by putting the points in a canonical configuration,

$$\phi_1 \leq 0, \quad \phi_1 \leq \phi_2 \leq -\phi_1, \quad 0 \leq \lambda_{12} \leq \pi. \quad (71)$$

This may be accomplished swapping the end points and the signs of the coordinates if necessary, and the solution may similarly be transformed to apply to the original points. Referring to Fig. 3, note that, with these orderings of the coordinates, all geodesics with $\alpha_1 \in [0, \pi]$ intersect latitude ϕ_2 with $\lambda_{12} \in [0, \pi]$. Furthermore, the search for solutions can be restricted to $\alpha_2 \in [0, \frac{1}{2}\pi]$, i.e., when the geodesic *first* intersects latitude ϕ_2 . (For $\phi_2 = -\phi_1$, there is a second shortest path with $\alpha_2 \in [\frac{1}{2}\pi, \pi]$ if λ_{12} is nearly equal to π . But this geodesic is easily derived from the first.)

Meridional geodesics are treated as a special case. These include the cases $\lambda_{12} = 0$ or π and $\beta_1 = -\frac{1}{2}\pi$ with any λ_{12} . This also includes the case where A and B are coincident. In these cases, set $\alpha_1 = \lambda_{12}$ and $\alpha_2 = 0$. (This value of α_1 is consistent with the prescription for azimuths near a pole given at the end of Sect. 6.)

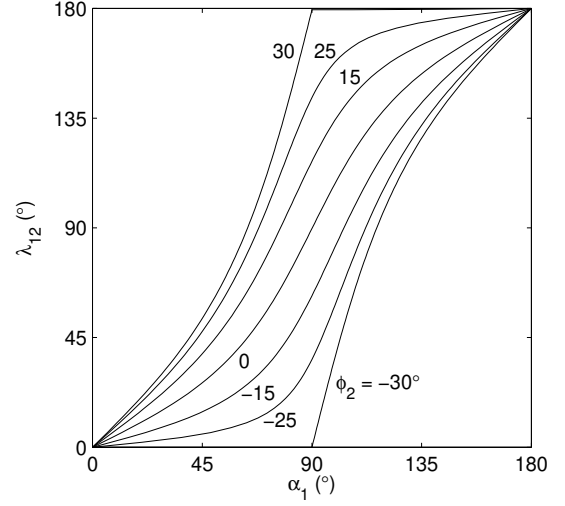


FIG. 6 The variation of λ_{12} as a function of α_1 . The latitudes are $\phi_1 = -30^\circ$ and $\phi_2 = -30^\circ, -25^\circ, -15^\circ, 0^\circ, 15^\circ, 25^\circ, 30^\circ$. For $\phi_1 < 0$ and $\phi_1 < \phi_2 < -\phi_1$, the curves are strictly increasing, while for $\phi_1 < 0$ and $\phi_2 = \pm\phi_1$, the curves are non-decreasing with discontinuities in the slopes at $\alpha_1 = 90^\circ$ (see Fig. 7). The WGS84 ellipsoid is used.

Define now a variant of the direct geodesic problem: given ϕ_1, ϕ_2 , subject to Eq. (71), and α_1 , find λ_{12} . Proceed as in the direct problem up to the solution of the triangle NEA . Find β_2 from Eq. (8) and solve the triangle NEB for $\alpha_2 \in [0, \frac{1}{2}\pi]$, σ_2, ω_2 from Eqs. (9), (14), and (10). Finally, determine λ_{12} as in the solution to the direct problem. In determining α_2 from Eq. (9), I use in addition

$$\cos \alpha_2 = \frac{+\sqrt{\cos^2 \alpha_1 \cos^2 \beta_1 + (\cos^2 \beta_2 - \cos^2 \beta_1)}}{\cos \beta_2}, \quad (72)$$

where the parenthetical term under the radical is computed by $(\cos \beta_2 - \cos \beta_1)(\cos \beta_2 + \cos \beta_1)$ if $\beta_1 < -\frac{1}{4}\pi$ and by $(\sin \beta_1 - \sin \beta_2)(\sin \beta_1 + \sin \beta_2)$ otherwise. It remains to determine the value of α_1 that results in the given value of λ_{12} .

I show the behavior of λ_{12} as a function of α_1 in Figs. 6–7. For an oblate ellipsoid and $|\beta_2| < -\beta_1$, λ_{12} is a strictly increasing function of α_1 . For $\beta_2 = \beta_1$, λ_{12} vanishes for $0 \leq \alpha_1 < \frac{1}{2}\pi$; for $\beta_2 = -\beta_1$, $d\lambda_{12}/d\alpha_1$ vanishes for $\alpha_1 = \frac{1}{2}\pi+$. Therefore if $\beta_1 = \beta_2 = 0$, λ_{12} is discontinuous at $\alpha_1 = \frac{1}{2}\pi$ jumping from 0 to $(1-f)\pi$. This is the case of equatorial end points—if $\lambda_{12} \leq (1-f)\pi$, the geodesic lies along the equator, with $\alpha_1 = \alpha_2 = \frac{1}{2}\pi$.

Thus with the ordering given by Eq. (71), simple root finding methods, such as binary search or *regula falsi*, will allow α_1 to be determined for a given λ_{12} . Because such methods converge slowly, I instead solve for α_1 using Newton's method.

First, I compute the necessary derivative. Consider a trial geodesic with initial azimuth α_1 . If the azimuth is increased to $\alpha_1 + d\alpha_1$ with the length held fixed, then the other end of the geodesic moves by $m_{12} d\alpha_1$ in a direction $\frac{1}{2}\pi + \alpha_2$. If the

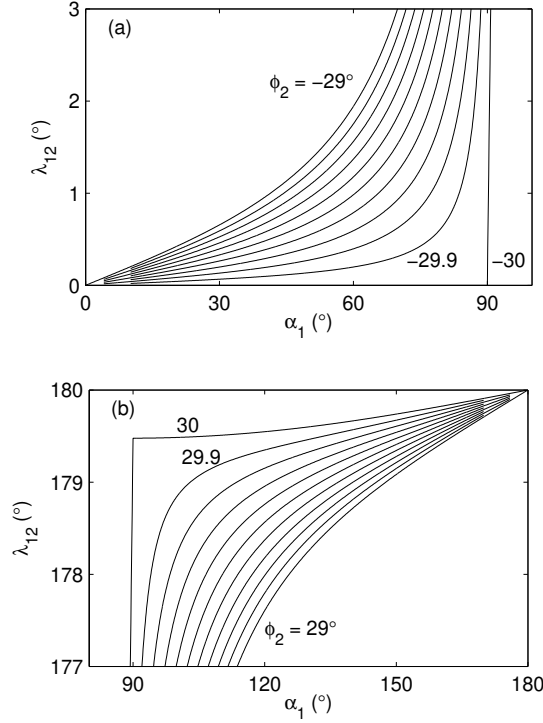


FIG. 7 Details of λ_{12} as a function of α_1 near the discontinuities in the slopes. This shows blow-ups of the two “corner” regions in Fig. 6 (for $\phi_1 = -30^\circ$). (a) The short line limit, where $\phi_2 \approx \phi_1$ and $\lambda_{12} \approx 0$; here, ϕ_2 is in $[-30^\circ, -29^\circ]$ at intervals of 0.1° . At $\phi_2 = \phi_1 = -30^\circ$ and $\alpha_1 = 90^\circ$, the slope changes from zero to a finite value. (b) The nearly antipodal limit, where $\phi_2 \approx -\phi_1$ and $\lambda_{12} \approx 180^\circ$; here, ϕ_2 is in $[29^\circ, 30^\circ]$ at intervals of 0.1° . At $\phi_2 = -\phi_1 = 30^\circ$ and $\alpha_1 = 90^\circ$, the slope changes from a finite value to zero.

geodesic is extended to intersect the parallel ϕ_2 once more, the point of intersection moves by $m_{12} d\alpha_1 / \cos \alpha_2$; see Fig. 8. The radius of this parallel is $a \cos \beta_2$, thus the rate of change of the longitude difference is

$$\left. \frac{d\lambda_{12}}{d\alpha_1} \right|_{\phi_1, \phi_2} = \frac{m_{12}}{a} \frac{1}{\cos \alpha_2 \cos \beta_2}, \quad (73)$$

where the subscripts on the derivative indicate which quantities are held fixed in taking the derivative. The denominator can vanish if $\beta_2 = |\beta_1|$ and $\alpha_2 = \frac{1}{2}\pi$; in this case, use

$$\left. \frac{d\lambda_{12}}{d\alpha_1} \right|_{\phi_1, \phi_2} = -\frac{\sqrt{1 - e^2 \cos^2 \beta_1}}{\sin \beta_1} (1 \mp \text{sign}(\cos \alpha_1)), \quad (74)$$

for $\beta_2 = \pm\beta_1$. For Newton’s method, pick the positive derivative, i.e., take $1 \mp \text{sign}(\cos \alpha_1) = 2$, which corresponds to $\alpha_1 = 90^\circ \pm$ for $\phi_2 = \pm\phi_1$ in Fig. 6.

Newton’s method requires a sufficiently accurate starting guess for α_1 to converge. To determine this, I first estimate ω_{12} , the longitude difference on the auxiliary sphere, and then find α_1 using Eq. (68). To obtain this estimate for ω_{12} , I distinguish three regions; see Fig. 9 (the caption gives the precise

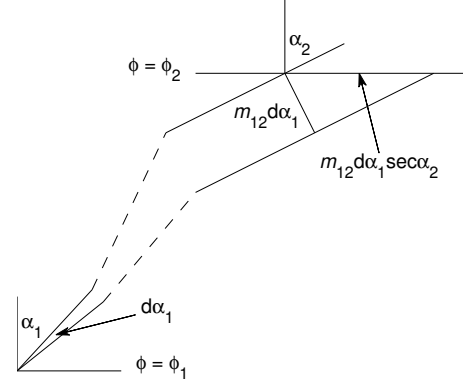


FIG. 8 Finding $d\lambda_{12}/d\alpha_1$ with ϕ_1 and ϕ_2 held fixed.

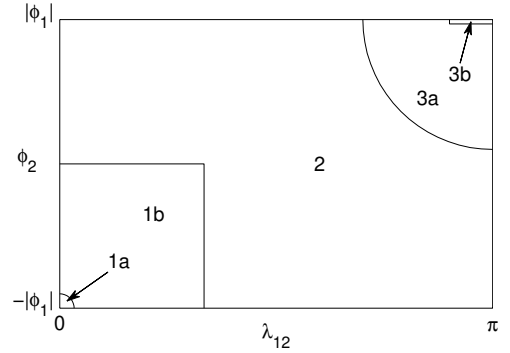


FIG. 9 Schematic showing the 5 regions for the inverse problem. Region 1 is given by $\lambda_{12} < \frac{1}{6}\pi$ and $\beta_2 - \beta_1 < \frac{1}{6}\pi$. Region 1a is given by $\sigma_{12} < \sqrt{\delta}/\max(0.1, |e^2|)$. Region 3 is given by $\sigma_{12} > \pi(1 - 3|f|A_3 \cos^2 \beta_1)$. Region 3b is given by $y > -100\delta$ and $x > -1 - 1000\sqrt{\delta}$.

boundaries of the regions). (1) Short lines: If λ_{12} and $\beta_2 - \beta_1$ are reasonably small, then use $\omega_{12} \approx \lambda_{12}/w_1$, where w_1 is given by Eq. (20). (2) Intermediate lines: Assume $\omega_{12} = \lambda_{12}$, provided that the resulting σ_{12} is sufficiently less than π . (3) Long lines: Analyze the problem using the methods of Sect. 7, evaluate $x < 0$ and $y \leq 0$, and use Eq. (67) as an estimate of ω_{12} . However, if y is very small and $-1 \leq x \leq 0$, then ω_{12} is nearly equal to π and Eq. (68) becomes indeterminate; in this case, estimate α_1 directly using $\alpha_1 \approx \theta + \frac{1}{2}\pi$, with θ given by Eq. (66) (region 3b in Fig. 9). This rule is also applied for x slightly less than -1 , to ensure that Newton’s method doesn’t get tripped by the discontinuity in the slope of $\lambda_{12}(\alpha_1)$ in Fig. 7b.

This provides suitable starting values for α_1 for use in Newton’s method. Carrying out Newton’s method can be avoided in case 1 above if σ_{12} , Eq. (70), is sufficiently small (case 1a in Fig. 9), in which case the full solution is given by Eqs. (68)–(70) with $s_{12} = aw_1\sigma_{12}$. This also avoids the problem of maintaining accuracy when solving for λ_{12} given $\phi_2 \approx \phi_1$ and $\alpha_1 \approx \frac{1}{2}\pi$. Details of the convergence of Newton’s method

are given in Sect. 9. The boundaries of regions 1a and 3b in Fig. 9 depend on the precision of the floating-point number system. This is characterized by $\delta = 1/2^{p-1}$ where p is the number of bits of precision in the number system and $1 + \delta$ is the smallest representable number greater than 1. Typically $p = 53$ and $\delta = 2.2 \times 10^{-16}$ for double precision.

Once a converged value of α_1 has been found, converged values of α_2 , σ_1 , and σ_2 are also known (during the course of the final Newton iteration), and s_{12} can be found using Eq. (33). The quantities m_{12} , M_{12} , and M_{21} can also be computed as in the solution of the direct problem. This completes the solution of the inverse problem for an ellipsoid.

In the following cases, there are multiple solutions to the inverse problem and I indicate how to find them all given one solution. (1) If $\phi_1 + \phi_2 = 0$ (and neither point is at the pole) and if $\alpha_1 \neq \alpha_2$, a second geodesic is obtained by setting $\alpha_1 = \alpha_2$ and $\alpha_2 = \alpha_1$. (This occurs when $\lambda_{12} \approx \pm 180^\circ$ for oblate ellipsoids.) (2) If $\lambda_{12} = \pm 180^\circ$ (and neither point is at a pole) and if the geodesic is not meridional, a second geodesic is obtained by setting $\alpha_1 = -\alpha_1$ and $\alpha_2 = -\alpha_2$. (This occurs when the $\phi_1 + \phi_2 \approx 0$ for prolate ellipsoids.) (3) If A and B are at opposite poles, there are infinitely many geodesics which can be generated by setting $\alpha_1 = \alpha_1 + \gamma$ and $\alpha_2 = \alpha_2 - \gamma$ for arbitrary γ . (For spheres, this prescription applies when A and B are antipodal.) (4) If $s_{12} = 0$ (coincident points), there are infinitely many geodesics which can be generated by setting $\alpha_1 = \alpha_1 + \gamma$ and $\alpha_2 = \alpha_2 + \gamma$ for arbitrary γ .

The methods given here can be adapted to return geodesics which are not shortest paths provided a suitable starting point for Newton’s method is given. For example, geodesics 2–4 in Table 1 can be found by using the negative square root in the equation for $\cos \alpha_2$, Eq. (72); and for geodesic 4, solve the problem with $2\pi - \lambda_{12} = 180.2^\circ$ as the longitude difference. In these cases, the starting points are given by the multiple solutions of the astroid equation, Eq. (65). Geodesics that wrap around the globe multiple times can be handled similarly.

Although the published inverse method of Vincenty (1975a) fails to converge for nearly antipodal points, he did give a modification of his method that deals with this case (Vincenty, 1975b). The method requires one minor modification: following his Eq. (10), insert $\cos \sigma = -\sqrt{1 - \sin^2 \sigma}$. The principal drawback of his method (apart from the limited accuracy of his series) is its very slow convergence for nearly conjugate points—in some cases, many thousands of iterations are required. In contrast, by using Newton’s method, the method described here converges in only a few iterations. Sodano (1958), starting with the same formulation as given here (Bessel, 1825; Helmert, 1880) derives an approximate non-iterative solution for the inverse problem; however, this may fail for antipodal points (Rapp, 1993, §1.3). Sodano’s justification for his method is illuminating: a non-iterative method is better suited to the mechanical and electronic computers of his day. (See also my comment about Vincenty’s use of programmable calculators at the end of Sect. 5.) The situation now is, of course, completely different: the series of Bessel and Helmert are readily implemented on modern computers and iterative methods are frequently key to efficient and accurate computational algorithms.

TABLE 2 Truncation errors for the main geodesic problems. Δ_d and Δ_i are approximate upper bounds on the truncation errors for the direct and inverse problems. The parameters of the WGS84 and the SRMmax ellipsoids are used. The SRMmax ellipsoid, $a = 6400$ km, $f = 1/150$, is an ellipsoid with an exaggerated flattening introduced by the National Geospatial-Intelligence Agency for the purposes of algorithm testing.

L	WGS84		SRMmax	
	Δ_d (m)	Δ_i (m)	Δ_d (m)	Δ_i (m)
2	2.6×10^{-2}	2.6×10^{-2}	2.1×10^{-1}	2.1×10^{-1}
3	3.7×10^{-5}	1.6×10^{-5}	5.8×10^{-4}	2.5×10^{-4}
4	1.1×10^{-7}	3.2×10^{-8}	3.3×10^{-6}	1.0×10^{-6}
5	2.5×10^{-10}	2.3×10^{-11}	1.6×10^{-8}	1.5×10^{-9}
6	7.7×10^{-13}	5.3×10^{-14}	9.6×10^{-11}	6.6×10^{-12}
7	2.1×10^{-15}	4.1×10^{-17}	5.2×10^{-13}	1.0×10^{-14}
8	6.8×10^{-18}	1.1×10^{-19}	3.4×10^{-15}	5.0×10^{-17}
9	2.0×10^{-20}	8.0×10^{-23}	2.0×10^{-17}	7.9×10^{-20}
10	6.6×10^{-23}	2.1×10^{-25}	1.3×10^{-19}	4.1×10^{-22}
12	6.7×10^{-28}	4.6×10^{-31}	5.2×10^{-24}	3.6×10^{-27}
14	7.0×10^{-33}	1.1×10^{-36}	2.2×10^{-28}	3.3×10^{-32}
16	7.7×10^{-38}	2.5×10^{-42}	9.4×10^{-33}	3.0×10^{-37}
18	8.5×10^{-43}	5.8×10^{-48}	4.2×10^{-37}	2.8×10^{-42}
20	9.7×10^{-48}	1.4×10^{-53}	1.9×10^{-41}	2.7×10^{-47}

9. ERRORS

Floating-point implementations of the algorithms described in Secs. 6 and 8 are included in GeographicLib (Karney, 2010). These suffer from two sources of error: truncation errors because the series in Sect. 5, when truncated at order L , differ from the exact integrals; and round-off errors due to evaluating the series and solving the resulting problem in spherical trigonometry using inexact (floating-point) arithmetic. In order to assess both types of error, it is useful to be able to compute geodesics with arbitrary accuracy. For this purpose, I used Maxima’s Taylor package to expand the series to 30th order and its “bigfloat” package to solve the direct problem with 100 decimal digits. The results obtained in this way are accurate to at least 50 decimal digits and may be regarded as “exact”.

I first present the truncation errors. I carry out a sequence of direct geodesic computations with random ϕ_1 , α_1 , and s_{12} (subject to the shortest path constraint) comparing the position of the end point (ϕ_2 and λ_{12}) computed using the series truncated to order L with the exact result (i.e., with $L = 30$), in both cases using arithmetic with 100 decimal digits. The results are shown in Table 2 which shows the approximate maximum truncation error as a function of $L \leq 20$. The quantity Δ_d gives the truncation error for the method as given in Sect. 6; this scales as f^L . On the other hand, Δ_i is the truncation error where, instead of solving σ in terms of s using the truncated reverted series, Eq. (56), I invert the truncated series for s , Eqs. (33) and (43), to give σ in terms of s . (This is done “exactly”, i.e., using Newton’s method and demanding

convergence to 100 decimal places.) This is representative of the truncation error in the solution of inverse geodesic problem, because the inverse problem does not involve determining σ in terms of s . Δ_i scales approximately as $(\frac{1}{2}f)^L$. For comparison, the truncation errors for Vincenty's algorithm are 9.1×10^{-5} m and 1.5×10^{-3} m for the WGS84 and SRMmax ellipsoids; these errors are about 2.5 times larger than Δ_d for $L = 3$ (the order of Vincenty's series).

I turn now to the measurement of the round-off errors. The limiting accuracy, assuming that the fraction of the floating-point representation contains $p = 53$ bits, is about $20\,000 \text{ km}/2^{53} \approx 2 \text{ nm}$ (where $20\,000 \text{ km}$ is approximately half the circumference of the earth). From Table 2, the choice $L = 6$ ensures that the truncation error is negligible compared to the round-off error even for $f = 1/150$. I assembled a large set of exact geodesics for the WGS84 ellipsoid to serve as test data. These were obtained by solving the direct problem using Maxima using the protocol described at the beginning of this section. All the test data satisfies $\sigma_{12} \leq 180^\circ$, so that they are all shortest paths. Each test geodesic gives accurate values for ϕ_1 , α_1 , ϕ_2 , λ_{12} , s_{12} , σ_{12} , and m_{12} . In this list ϕ_1 , α_1 , and s_{12} are "input" values for the direct problem. The other values are computed and then rounded to the nearest 0.1 μm in the case of m_{12} and $(10^{-18})^\circ$ in the case of the angles. The test data includes randomly chosen geodesics together with a large number of geodesics chosen to uncover potential numerical problems. These include nearly meridional geodesics, nearly equatorial ones, geodesics with one or both end points close to a pole, and nearly antipodal geodesics.

For each test geodesic, I use the floating-point implementations of the algorithms to solve the direct problem from each end point and to solve the inverse problem. Denoting the results of the computations with an asterisk, I define the error in a computed quantity x by $\delta x = x^* - x$. For the direct problem computed starting at the first end point, I compute the error in the computed position of the second end point as

$$|\rho_2 \delta \phi_2 + i \cos \phi_2 \nu_2 \delta \lambda_2|.$$

I convert the error in the azimuth into a distance via

$$a |\delta \alpha_2 - \delta \lambda_{12} \sin \phi_2|,$$

which is proportional to the error in the direction of the geodesic at B in three dimensions and accounts for the coupling of α_2 and λ_{12} near the poles. I compute the corresponding errors when solving the direct problem starting at the second end point.

For the inverse problem, I record the error in the length

$$|\delta s_{12}|.$$

I convert the errors in the azimuths into a length using

$$\max(|\delta \alpha_1|, |\delta \alpha_2|) |m_{12}|;$$

the multiplication by the reduced length accounts for the sensitivity of the azimuths to the positions of the end points. An obvious example of such sensitivity is when the two points are close to opposite poles or when they are very close to each

TABLE 3 Two close geodesics. The parameters of the WGS84 ellipsoid are used.

	Case 1	Case 2
ϕ_1		-30°
ϕ_2	30°	$(30 - 4 \times 10^{-15})^\circ$
λ_{12}	179.477 019 999 756 66 $^\circ$	
α_1	90.000 008 $^\circ$	90.001 489 $^\circ$
α_2	89.999 992 $^\circ$	89.998 511 $^\circ$
s_{12}	19 978 693.309 037 086 m	
σ_{12}	180 $^\circ$	180.000 000 $^\circ$
m_{12}	1.1 nm	51 μm

other. A less obvious case is illustrated in Table 3. The second end points in cases 1 and 2 are only 0.4 nm apart; and yet the azimuths in the two cases differ by $-5.3''$ and the two geodesics are separated by about 160 m at their midpoints. (This "unstable" case finding the conjugate point for a geodesic by solving the direct problem with $\alpha_1 = 90^\circ$ and spherical arc length of $\sigma_{12} = 180^\circ$.)

This provides a suitable measure of the *accuracy* of the computed azimuths for the inverse problem. I also check their *consistency*. If $s_{12} \geq a$, I determine the midpoint of the computed geodesic by separate direct geodesic calculations starting at either end point with the respective computed azimuths and geodesic lengths $\pm \frac{1}{2} s_{12}^*$ and I measure the distance between the computed midpoints. Similarly for shorter geodesics, $s_{12} < a$, I compare the computed positions of a point on the geodesic a distance a beyond the second point with separate direct calculations from the two endpoints and repeat such a comparison for a point a distance a before the first end point.

In this way, all the various measures of the accuracy of the direct and inverse geodesic are converted into comparable ground distances, and the maximum of these measures over a large number of test geodesics is a good estimate of the combined truncation and round-off errors for the geodesic calculations. The maximum error using double precision ($p = 53$) is about 15 nm. With extended precision ($p = 64$), the error is about 7 μm , consistent with 11 bits of additional precision. The test data consists of geodesics which are shortest paths, the longest of which is about 20 000 km. If the direct problem is solved for longer geodesics (which are not therefore shortest paths), the error grows linearly with length. For example, the error in a geodesic of length 200 000 km that completely encircles the earth 5 times is about 150 nm (for double precision).

Another important goal for the test set was to check the convergence of the inverse solution. Usually a practical convergence criterion for Newton's method is that the relative change in the solution is less than $O(\sqrt{\delta})$; because of the quadratic convergence of the method, this ensures that the error in the solution is less than $O(\delta)$. However, this reasoning breaks down for the inverse geodesic problem because the deriva-

TABLE 4 Ellipsoidal trigonometry problems. Here, ξ , ζ , and θ are the three given quantities. The “notes” column gives the number assigned by Oriani (1810, p. 48) in his “index of spheroidal problems” and by Puissant (1831, p. 521) in his enumeration of solutions. See the text for an explanation of the other columns.

No.	ξ, ζ, θ	ψ	Ref.	$\left. \frac{d\theta}{d\psi} \right _{\xi, \zeta}$	Notes
1	ϕ_1, α_1, ϕ_2				1, 1
2	$\phi_1, \alpha_1, \alpha_2$				3, 12
3	ϕ_1, α_1, s_{12}	σ_{12}		Eq. (75)	5, 2
4	$\phi_1, \alpha_1, \lambda_{12}$	σ_{12}		Eq. (76)	11, 6
5	ϕ_1, ϕ_2, s_{12}	α_1	1	Eq. (77)	7, 3
6	$\phi_1, \phi_2, \lambda_{12}$	α_1	1	Eq. (78)	13, 7
7	ϕ_1, α_2, s_{12}	α_1	2	Eq. (79)	8, 4
8	$\phi_1, \alpha_2, \lambda_{12}$	α_1	2	Eq. (80)	14, 8
9	$\phi_1, s_{12}, \lambda_{12}$	α_1	3	Eq. (81)	19, 11
10	$\alpha_1, s_{12}, \lambda_{12}$	ϕ_1	3	Eq. (82)	17, 10
11	$\alpha_1, \alpha_2, s_{12}$	ϕ_1	2	Eq. (83)	10, 5
12	$\alpha_1, \alpha_2, \lambda_{12}$	ϕ_1	2	Eq. (84)	16, 9

tive of λ_{12} with respect to α_1 can become arbitrarily small; therefore a more conservative convergence criterion is used. Typically 2–4 iterations of Newton’s method are required. A small fraction of geodesics, those with nearly conjugate end points, require up to 16 iterations. No convergence failures are observed.

10. ELLIPSOIDAL TRIGONOMETRY

The direct and inverse geodesic problems are two examples of solving the ellipsoidal triangle NAB in Fig. 1 given two sides and the included angle. The sides of this triangle are given by $NA = aE(\frac{1}{2}\pi - \beta_1, e)$, $NB = aE(\frac{1}{2}\pi - \beta_2, e)$, and $AB = s_{12}$ and its angles are $NAB = \alpha_1$, $NBA = \pi - \alpha_2$, and $ANB = \lambda_{12}$. The triangle is fully solved if $\phi_1, \alpha_1, \phi_2, \alpha_2, s_{12}$, and λ_{12} are all known. The typical problem in ellipsoidal trigonometry is to solve the triangle if just three of these quantities are specified. Considering that A and B are interchangeable, there are 12 distinct such problems which are laid out in Table 4. (In plane geometry, there are four distinct triangle problems. On a sphere, the constraint on the sum of the angles of a triangle is relaxed, leading to six triangle problems.)

Oriani (1810, p. 48) and Puissant (1831, p. 521) both gave similar catalogs of ellipsoidal problems as Table 4. Here (and in Sect. 11), I do not give the full solution of the ellipsoidal problems nor do I consider how to distinguish the cases where there may be 0, 1, or 2 solutions. Instead, I indicate how, in each case, an accurate solution may be obtained using Newton’s method assuming that a sufficiently accurate starting guess has been found. This might be obtained by approximating the ellipsoid by a sphere and using spherical trigonometry (Todhunter, 1871, Chap. 6) or by using approximate ellip-

soidal methods (Rapp, 1991, §6). In Sect. 13, I also show how the gnomonic projection may be used to solve several ellipsoidal problems using plane geometry.

In treating these problems, recall that the relation between ϕ and β is given by Eq. (8) and depends only on the eccentricity of the ellipsoid. On the other hand, the relations between s_{12} and λ_{12} and the corresponding variables on the auxiliary sphere, σ_{12} and ω_{12} , depend on the geodesic (specifically on α_0).

In Table 4, ξ, ζ, θ are the given quantities. In problems 1 and 2, the given quantities are all directly related to corresponding quantities for the triangle on the auxiliary sphere. This allows the auxiliary triangle to be solved and the ellipsoidal quantities can then be obtained. (Problem 1 was used in solving the inverse problem in Sect. 8.)

Problem 3 is the direct problem whose solution is given in Sect. 6. Here, however, I give the solution by Newton’s method to put this problem on the same footing as the other problems. The solution consists of treating σ_{12} (the column labeled ψ) as a “control variable”. Assume a value for this quantity, solve the problem with given $\phi_1, \alpha_1, \sigma_{12}$ (i.e., ξ, ζ, ψ) for s_{12} (i.e., θ) using Eq. (33). The value thus found for s_{12} will, of course, differ from the given value and a better approximation for σ_{12} is found using Newton’s method with

$$\left. \frac{ds_{12}}{d\sigma_{12}} \right|_{\phi_1, \alpha_1} = aw_2. \quad (75)$$

The equation for the derivative needed for Newton’s method is given in the column labeled $d\theta/d\psi|_{\xi, \zeta}$ in the table. Problem 4 is handled similarly except that Eq. (35) is used to give λ_{12} and the necessary derivative for Newton’s method is

$$\left. \frac{d\lambda_{12}}{d\sigma_{12}} \right|_{\phi_1, \alpha_1} = \frac{w_2 \sin \alpha_2}{\cos \beta_2}. \quad (76)$$

Problems 1–4 are the simplest ellipsoidal trigonometry problems with ϕ and α specified at the same point, so that it is possible to determine α_0 which fixes the relation between s_{12} and σ_{12} and between λ_{12} and ω_{12} . In the remaining problems it is necessary to assume a value for ϕ_1 or α_1 thereby reducing the problem to one of the reference problems 1–3 (the column labeled “Ref.”). Thus, given ξ, ζ, θ , assume a value $\psi^{(0)}$ for ψ ; solve the reference problem $\xi, \zeta, \psi^{(i)}$ to determine $\theta^{(i)}$; find a more accurate approximation to ψ using

$$\psi^{(i+1)} = \psi^{(i)} - (\theta^{(i)} - \theta) \left(\left. \frac{d\theta^{(i)}}{d\psi^{(i)}} \right|_{\xi, \zeta} \right)^{-1},$$

and iterate until convergence. The remaining derivatives are

$$\left. \frac{ds_{12}}{d\alpha_1} \right|_{\phi_1, \phi_2} = m_{12} \tan \alpha_2, \quad (77)$$

$$\left. \frac{d\lambda_{12}}{d\alpha_1} \right|_{\phi_1, \phi_2} = \frac{m_{12}}{a} \frac{1}{\cos \alpha_2 \cos \beta_2}, \quad (78)$$

$$\left. \frac{ds_{12}}{d\alpha_1} \right|_{\phi_1, \alpha_2} = m_{12} \tan \alpha_2 - \frac{aw_2}{\tan \alpha_1 \tan \beta_2 \cos \alpha_2}, \quad (79)$$

$$\left. \frac{d\lambda_{12}}{d\alpha_1} \right|_{\phi_1, \alpha_2} = \frac{m_{12}/a}{\cos \alpha_2 \cos \beta_2} - \frac{w_2 \tan \alpha_2}{\tan \alpha_1 \sin \beta_2}, \quad (80)$$

$$\left. \frac{d\lambda_{12}}{d\alpha_1} \right|_{\phi_1, s_{12}} = \frac{m_{12} \cos \alpha_2}{a \cos \beta_2}, \quad (81)$$

$$\left. \frac{d\lambda_{12}}{d\phi_1} \right|_{\alpha_1, s_{12}} = \frac{w_1^3}{(1-f) \sin \alpha_1} \times \left(\frac{\cos \alpha_1}{\cos \beta_1} - \frac{\cos \alpha_2}{\cos \beta_2} N_{12} \right), \quad (82)$$

$$\left. \frac{ds_{12}}{d\phi_1} \right|_{\alpha_1, \alpha_2} = a \frac{w_1^3}{1-f} \left(-\frac{N_{12} \tan \alpha_2}{\sin \alpha_1} + \frac{\tan \beta_1}{\cos \alpha_2 \tan \beta_2} \frac{w_2}{w_1} \right), \quad (83)$$

$$\left. \frac{d\lambda_{12}}{d\phi_1} \right|_{\alpha_1, \alpha_2} = \frac{w_1^3}{1-f} \left(\frac{\cos \alpha_1}{\sin \alpha_1 \cos \beta_1} - \frac{N_{12} \sec \alpha_2}{\sin \alpha_1 \cos \beta_2} + \frac{\tan \beta_1 \tan \alpha_2}{\sin \beta_2} \frac{w_2}{w_1} \right), \quad (84)$$

where

$$N_{12} = M_{12} - \frac{(m_{12}/a) \cos \alpha_1 \tan \beta_1}{w_1}.$$

The choice of ψ in these solutions is somewhat arbitrary; other choices may be preferable in some cases. These formulas for the derivatives are obtained with constructions similar to Fig. 8. Equations (82)–(84) involve partial derivatives taken with α_1 held constant; the role of N_{12} in these equation can be contrasted with that of M_{12} as follows. Consider a geodesic from A to B with length s_{12} and initial azimuth α_1 . Construct a second geodesic of the same length from A' to B' where A' is given by moving a small distance dt from A in a direction $\alpha_1 + \frac{1}{2}\pi$. If the initial direction of the second geodesic is $\alpha'_1 = \alpha_1$ (resp. parallel to the first geodesic), then the distance from B to B' is $N_{12} dt$ (resp. $M_{12} dt$). (Because meridians converge, two neighboring geodesics with the same azimuth are not, in general, parallel.)

Problem 6 is the geodesic inverse problem solved in Sect. 8 and I have repeated Eq. (73) as Eq. (78). Problem 7 is the “retro-azimuthal” problem for which Hinks (1929) gives an interesting application. For many years a radio at Rugby transmitted a long wavelength time signal. Hinks’ retro-azimuthal problem is to determine the position of an unknown point with knowledge of the distance and bearing to Rugby.

11. TRIANGULATION FROM A BASELINE

The ellipsoidal triangle considered in Sect. 10 is special in that one of its vertices is a pole so that two of its sides are meridians. The next class of ellipsoidal problems treated is solving a triangle ABC with a known baseline, see Fig. 10a. Here, the goal is to determine the position of C if the positions if A and B are known, i.e., if ϕ_1 , ϕ_2 , and λ_{12} are given (and hence, from the solution of the inverse problem for AB , the quantities α_1 , α_2 , and s_{12} are known). This corresponds to a

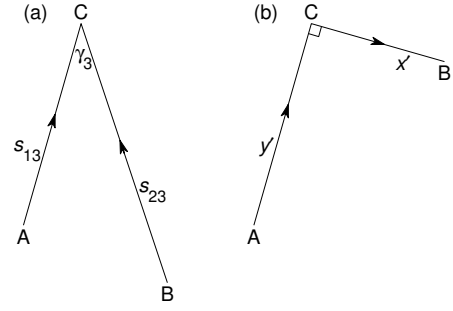


FIG. 10 Two ellipsoidal triangle problems: (a) triangulating from a baseline and (b) rectangular geodesic (or oblique Cassini–Soldner) coordinates.

TABLE 5 Ellipsoidal triangulation problems. In these problems, the positions of A and B (i.e., ϕ_1 , ϕ_2 , and λ_{12}) are given and the position of C is sought. The quantities ξ and ζ are the additional given quantities.

No.	ξ, ζ	ψ	$\left. \frac{d\zeta}{d\psi} \right _{\xi}$
0	$\alpha_{1(3)}, s_{13}$		
1	s_{13}, s_{23}	$\alpha_{1(3)}$	Eq. (85)
2	$\alpha_{1(3)}, \alpha_{2(3)}$	s_{13}	Eq. (86)
3	$\alpha_{1(3)}, s_{23}$	s_{13}	Eq. (87)
4	s_{13}, γ_3	$\alpha_{1(3)}$	Eq. (88)
5	$\alpha_{1(3)}, \gamma_3$	s_{13}	Eq. (89)

class of triangulation problems encountered in field surveying: a line AB is measured and is used as the base of a triangulation network. However, in the present context, A need not be visible from B and I consider both the problems of triangulation and trilateration. (In addition, remember that the angles measured by a theodolite are not the angles between geodesics but between normal sections.)

Because the problems entail consideration of more than a single general geodesic, it is necessary to generalize the notation for azimuthal angles to make clear which geodesic line is being measured. I define $\alpha_{i(j)}$ as the azimuth of the geodesic line passing through point i where j is some other point on the same line. Each geodesic line is assigned a unique direction, indicated by arrows in the figures, and all azimuths are forward azimuths (as before).

With one side specified and two additional quantities needed to solve the triangle, there are 10 possible problems to solve. Of these, six are distinct (considering the interchangeability of A and B) and are listed in Table 5. For the angle at C , I assume that $\gamma_3 = \alpha_{3(1)} - \alpha_{3(2)}$, the difference in the bearings of A and B , is given; this is included angle at C in Fig. 10a. In other words, I do not presume that the direction of due north is known, *a priori*, at C . This is the common situation with theodolite readings and it also includes the important case where γ is required to be $\pm \frac{1}{2}\pi$ which allows the

shortest distance from a point to a geodesic to be determined.

Problem 0 is just the direct geodesic problem (problem 3 of Sect. 10). The remaining 5 problems may be solved by Newton's method, in a similar fashion as in Sect. 10, as follows: replace the second given quantity ζ by one of the unknowns ψ ; estimate a value of ψ ; solve the problem with ξ and ψ (which, in each case, is a direct geodesic problem from A) to determine a trial position for C ; solve the inverse geodesic problem between B and the trial position for C to obtain a trial value for ζ ; update the value of ψ using Newton's method so that the resulting value of ζ matches the given value. The derivatives necessary for Newton's method are given in Eqs. (85)–(89):

$$\left. \frac{ds_{23}}{d\alpha_{1(3)}} \right|_{\phi_1, \phi_2, \lambda_{12}, s_{13}} = -m_{13} \sin \gamma_3, \quad (85)$$

$$\left. \frac{d\alpha_{2(3)}}{ds_{13}} \right|_{\phi_1, \phi_2, \lambda_{12}, \alpha_{1(3)}} = \frac{1}{m_{23}} \sin \gamma_3, \quad (86)$$

$$\left. \frac{ds_{23}}{ds_{13}} \right|_{\phi_1, \phi_2, \lambda_{12}, \alpha_{1(3)}} = \cos \gamma_3, \quad (87)$$

$$\left. \frac{d\gamma_3}{d\alpha_{1(3)}} \right|_{\phi_1, \phi_2, \lambda_{12}, s_{13}} = M_{31} - M_{32} \frac{m_{13}}{m_{23}} \cos \gamma_3, \quad (88)$$

$$\left. \frac{d\gamma_3}{ds_{13}} \right|_{\phi_1, \phi_2, \lambda_{12}, \alpha_{1(3)}} = \frac{M_{32}}{m_{23}} \sin \gamma_3. \quad (89)$$

The triangulation problems 1, 2, and 3, entail specification of either the distance or the bearing to C from each of A and B . These can also be solved by generalizing the method given by Sjöberg (2002, §5) for the solution of problem 2. The technique is to treat the latitude of C , ϕ_3 , as the control variable. Thus, start with an estimate for ϕ_3 ; if the bearing of (resp. distance to) C from a base point is given, then solve the intermediate problem $\phi_i, \phi_3, \alpha_{i(3)}$ (resp. s_{i3}) where $i = 1$ or 2 for base points A or B , i.e., problem 1 (resp. 5) in Sect. 10 to give λ_{i3} ; and evaluate $\lambda_{12} = \lambda_{13} - \lambda_{23}$. Now adjust ϕ_3 using Newton's method so that the λ_{12} matches the known value using

$$\left. \frac{d\lambda_{i3}}{d\phi_3} \right|_{\phi_i, \alpha_{i(3)}} = \frac{w_3^3 \tan \alpha_{3(i)}}{1 - f \cos \beta_3}, \quad (90)$$

$$\left. \frac{d\lambda_{i3}}{d\phi_3} \right|_{\phi_i, s_{i3}} = -\frac{w_3^3 \cot \alpha_{3(i)}}{1 - f \cos \beta_3}. \quad (91)$$

This method of solution essentially factors the problem into two simpler problems of the type investigated in Sect. 10.

A similar approach can also be applied to problem 5. Guess a value of s_{13} , solve problems 3 and 1 of Sect. 10 to determine successively the positions of C and B . Adjust s_{13} using Newton's method so that the correct value of λ_{12} is obtained, which requires the use of the derivative

$$\left. \frac{d\lambda_{12}}{ds_{13}} \right|_{\phi_1, \phi_2, \alpha_{1(3)}, \gamma_3} = -\frac{M_{32} \sin \gamma_3 \sec \alpha_{2(3)}}{a \cos \beta_2}. \quad (92)$$

Knowledge of reduced length and the geodesic scale allow errors to be propagated through a calculation. For example,

if the measurements of $\alpha_{1(3)}$ and $\alpha_{2(3)}$ are subject to an instrumental error $\delta\alpha$, then the error ellipse in the position of C when solving problem 2 will have a covariance which depends on $m_{13} \delta\alpha$, $m_{23} \delta\alpha$, and γ_3 . The effects of errors in the positions of A and B and in the measurements of s_{13} and s_{23} can be similarly estimated.

RNAV (2007, §§A2.4.1–3) also presents solution for problems 1–3. However, these use the secant method and so converge more slowly than the methods given here.

12. GEODESIC PROJECTIONS

Several map projections are defined in terms of geodesics. In the azimuthal equidistant projection (Snyder, 1987, §25) the distance and bearing from a central point A to an arbitrary point B is preserved. Gauss (1902, §19) lays out the problem for a general surface: the point B is projected to plane cartesian coordinates,

$$x = s_{12} \sin \alpha_1, \quad y = s_{12} \cos \alpha_1.$$

Bagratuni (1967, §16) calls these “geodetic polar coordinates”. Gauss (1902, §15) proves that the geodesics (lines of constant α_1) and the geodesic circles (lines of constant s_{12}), which, by construction, intersect at right angles in the projection, also intersect at right angles on the ellipsoid (see Sect. 3). The scale in the radial direction is unity, while the scale in the azimuthal direction is s_{12}/m_{12} ; the projection is conformal only at the origin. The forward and reverse projections are given by solving the inverse and direct geodesic problems. The entire ellipsoid maps to an approximately elliptical area, with the azimuthal scale becoming infinite at the two boundary points on the x axis. The projection can be continued beyond the boundary giving geodesics which are no longer shortest lines and negative azimuthal scales. Snyder (1987, p. 197) gives the formulas for this projection for the ellipsoid only for the case where the center point is a pole. For example, if A is at the north pole then the projection becomes

$$s_{12} = aE\left(\frac{1}{2}\pi - \beta_2, e\right), \quad m_{12} = a \cos \beta_2.$$

However, the method given here is applicable for any center point. The projection is useful for showing distances and directions from a central transportation hub.

Gauss (1902, §23) also describes another basic geodesic projection, called “right-angle spheroidal coordinates” by Bagratuni (1967, §17). Consider a reference geodesic passing through the point A at azimuth $\alpha_{1(3)}$. The reverse projection, B , of the point x, y is given by the following operations which are illustrated in Fig. 10b: resolve the coordinates into the directions normal and parallel to the initial heading of the reference geodesic,

$$\begin{aligned} x' &= \cos \alpha_{1(3)} x - \sin \alpha_{1(3)} y, \\ y' &= \sin \alpha_{1(3)} x + \cos \alpha_{1(3)} y; \end{aligned}$$

starting at A proceed along the reference geodesic a distance y' to C ; then proceed along the geodesic with azimuth

$\alpha_{3(2)} = \alpha_{3(1)} + \frac{1}{2}\pi$ a distance x' to point B . (Here, the “forward” direction on the geodesic CB is to the right of the reference geodesic AC which is the opposite of the convention in Sect. 11.) Gauss (1902, §16) proves that geodesics (lines of constant y') and the geodesic “parallels” (lines of constant x') intersect at right angles on the ellipsoid. At B , the scale in the x' direction is unity while the scale in the y' direction is $1/M_{32}$ which is unity on $x' = 0$; thus the projection is conformal on $x' = 0$. The definition of the mapping given here provides the prescription for carrying out the reverse projections. The forward projection is solved as follows: determine the point C on the reference geodesic which is closest to B (problem 5 of Sect. 11); set x' to the distance CB signed positive or negative according to whether B is to the right or left of the reference geodesic; set y' to the distance AC signed positive or negative according to whether C is ahead or behind A on the reference geodesic; finally transform the coordinate frame

$$\begin{aligned} x &= \cos \alpha_{1(3)} x' + \sin \alpha_{1(3)} y', \\ y &= -\sin \alpha_{1(3)} x' + \cos \alpha_{1(3)} y'. \end{aligned}$$

In the case where the reference geodesic is the equator, the projection is the ellipsoidal generalization of the so-called “equidistant cylindrical” projection (Snyder, 1987, §12). Solving for the point C is trivial; the coordinates are given by

$$x = a\lambda_{12}, \quad y = a(E(e) - E(\frac{1}{2}\pi - \beta_2, e)), \quad M_{32} = \cos \beta_2,$$

where $E(k)$ is the complete elliptic integral of the second kind (Olver *et al.*, 2010, §19.2(ii)); see also Bugayevskiy and Snyder (1995, §2.1.4). The whole ellipsoid is mapped to a rectangular region with the poles mapped to lines (where the scale in the x direction is infinite). If the reference geodesic is a “central” meridian, the projection is called “Cassini–Soldner” (Snyder, 1987, §13) and C may most simply be found by finding the midpoint of the geodesic BD where D is the reflection of B in the plane of the central meridian. This allows the Cassini–Soldner mapping to be solved accurately for the whole ellipsoid, in contrast to the series method presented in Snyder (1987, p. 95) which is only valid near the central meridian. The ellipsoid maps to an approximately rectangular region with the scale in the y direction divergent where the equator intersects the boundary. The Cassini–Soldner was widely used for large-scale maps until the middle of the 20th century when it was almost entirely replaced by the transverse Mercator projection (Snyder, 1987, §8). Tasks such as navigation and artillery aiming were much more easily accomplished with a conformal projection, such as transverse Mercator, compared to Cassini–Soldner with its unequal scales. The general case of this mapping may be termed the “oblique Cassini–Soldner” projection. Because the reference geodesic is not closed in this case, it is not convenient to use this projection for mapping the entire ellipsoid because there may be multiple candidates for C , the position on the reference geodesic closest to B .

The doubly equidistant projection has been used in small-scale maps to minimize the distortions of large land masses

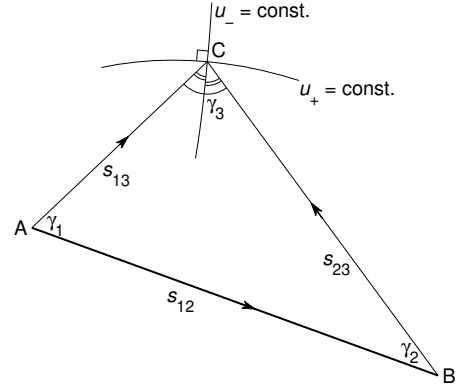


FIG. 11 The doubly equidistant projection. Also shown are portions of the geodesic ellipse and hyperbola through C .

(Bugayevskiy and Snyder, 1995, §7.9). In this projection, the distances to an arbitrary point C from two judiciously chosen reference points A and B are preserved; see Fig. 11. The formulas are usually given for a sphere; however, the generalization to an ellipsoid is straightforward. For the forward projection, fix the baseline AB with A and B separated by s_{12} ; solve the inverse geodesic problems for AC and BC and use the distances s_{13} and s_{23} together with elementary trigonometry to determine the position of C in the projected space; there are two solutions for the position of C either side of the baseline; the desired solution is the one that lies on the same side of the baseline as C on the ellipsoid. The reverse projection is similar, except that the position of C on the ellipsoid is determined by solving problem 1 in Sect. 11. The projection is only well defined if γ_1 and γ_2 are the same sign (consistent with a planar triangle). This is always the case for a sphere; the entire sphere projects onto an ellipse. However, on an ellipsoid, the geodesic connecting A and B is not closed in general and thus does not divide the ellipsoid into two halves. As a consequence, there may be a portion of the ellipsoid which is on one side of the baseline geodesic as seen from A but on the other side of it as seen from B ; such points cannot be projected. For example if $A = (35^\circ\text{N}, 40^\circ\text{E})$ and $B = (35^\circ\text{N}, 140^\circ\text{E})$, then the point $(43.5^\circ\text{S}, 60.5^\circ\text{W})$ cannot be projected because it is north of the baseline as seen by A but south of the baseline relative to B .

The scales of the doubly equidistant projection can be determined as follows. By construction, geodesic ellipses and hyperbolae, defined by $u_{\pm} = \frac{1}{2}(s_{13} \pm s_{23}) = \text{const.}$, map to ellipses and hyperbolae under this projection; see Fig. 11. Weingarten (1863) establishes these results for geodesic ellipses and hyperbolae (Eisenhart, 1909, §90): they are orthogonal; the geodesic hyperbola through C bisects the angle γ_3 made by the two geodesics from A and B ; and the scales in the u_{\pm} directions are $\cos \frac{1}{2}\gamma_3$ and $\sin \frac{1}{2}\gamma_3$, respectively. The same relations hold, of course, for the projected ellipses and hyperbolae, except that the angle ACB takes on a different (smaller) value γ'_3 . Thus, the elliptic and hyperbolic scale fac-

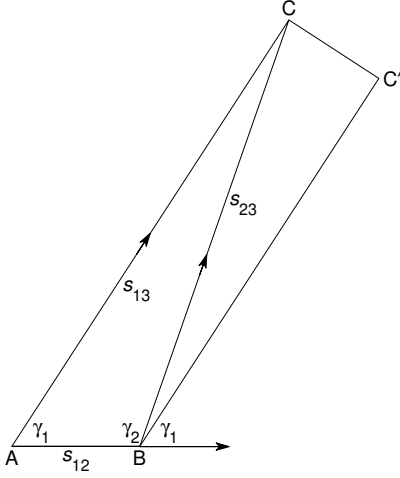


FIG. 12 The construction of the spheroidal gnomonic projection as the limit of a doubly azimuthal projection.

tors for the double equidistant projection may be written as

$$\frac{\cos \frac{1}{2}\gamma_3}{\cos \frac{1}{2}\gamma'_3}, \quad \frac{\sin \frac{1}{2}\gamma_3}{\sin \frac{1}{2}\gamma'_3},$$

respectively. Evaluating γ'_3 using the cosine rule for the plane triangle ABC' gives

$$\frac{2\sqrt{s_{13}s_{23}} \cos \frac{1}{2}\gamma_3}{\sqrt{(s_{13} + s_{23})^2 - s_{12}^2}}, \quad \frac{2\sqrt{s_{13}s_{23}} \sin \frac{1}{2}\gamma_3}{\sqrt{s_{12}^2 - (s_{13} - s_{23})^2}}.$$

The results generalize those of Cox (1946, 1951) for the projection of a sphere. In the limit $s_{12} \rightarrow 0$, this projection reduces to the azimuthal equidistant projection and these scales reduce to the radial scale, 1, and the azimuthal scale, s_{13}/m_{13} .

13. SPHEROIDAL GNOMONIC PROJECTION

The gnomonic projection of the sphere, which is obtained by a central projection of the surface of the sphere onto a tangent plane, has the property that all geodesics on the sphere map to straight lines (Snyder, 1987, §22). Such a projection is impossible for an ellipsoid because it does not have constant curvature (Beltrami, 1865). However, a spheroidal generalization of the gnomonic projections can be constructed for which geodesics are very nearly straight. First recall that the doubly azimuthal projection (Bugayevskiy and Snyder, 1995, §7.8) of the sphere, where the bearings from two points A and B to C are preserved, gives the gnomonic projection which is compressed in the direction parallel to AB . In the limit as B approaches A , the pure gnomonic projection is recovered.

The construction of the spheroidal gnomonic projection proceeds in the same way; see Fig. 12. Draw a geodesic BC' such that it is parallel to the geodesic AC at B . Its initial separation from AC is $s_{12} \sin \gamma_1$; at C' , the point closest to C , the separation becomes $M_{13}s_{12} \sin \gamma_1$ (in the limit

$s_{12} \rightarrow 0$). Thus the difference in the azimuths of the geodesics BC and BC' at B is $(M_{13}/m_{13})s_{12} \sin \gamma_1$, which gives $\gamma_1 + \gamma_2 = \pi - (M_{13}/m_{13})s_{12} \sin \gamma_1$. Now, solving the planar triangle problem with γ_1 and γ_2 as the two base angles gives the distance AC in the projected space as m_{13}/M_{13} .

Thus leads to the following specification for the spheroidal gnomonic projection. Let the center point be A ; for an arbitrary point B , solve the inverse geodesic problem between A and B ; then point B projects to the point

$$x = \rho \sin \alpha_1, \quad y = \rho \cos \alpha_1, \quad \rho = m_{12}/M_{12}; \quad (93)$$

the projection is undefined if $M_{12} \leq 0$. In the spherical limit, this becomes the standard gnomonic projection, $\rho = a \tan \sigma_{12}$ (Snyder, 1987, p. 165). The azimuthal scale is $1/M_{12}$ and the radial scale, found by computing $d\rho/ds_{12}$ and using Eq. (29), is $1/M_{12}^2$; the projection is therefore conformal at the origin. The reverse projection is found by $\alpha_1 = \text{ph}(y + ix)$ and by solving for s_{12} using Newton's method with $d\rho/ds_{12} = 1/M_{12}^2$ (i.e., the radial scale). Clearly the projection preserves the bearings from the center point and all lines through the center point are geodesics. Consider now a straight line BC in the projection and project this line on the spheroid. The distance that this deviates from a geodesic is, to lowest order,

$$h = \frac{l^2}{32}(\nabla K \cdot \mathbf{t})\mathbf{t}, \quad (94)$$

where l is the length of the geodesic, K is the Gaussian curvature, and \mathbf{t} is the perpendicular vector from the center of projection to the geodesic. I obtained this result semi-empirically: numerically, I determined that the maximum deviation was for east-west geodesics; I then found, by Taylor expansion, the deviation for the simple case in which the end points are equally distant from the center point at bearings $\pm\alpha$; finally, I generalized the resulting expression and confirmed this numerically. The deviation in the azimuths at the end points is about $4h/l$ and the length is greater than the geodesic distance by about $\frac{8}{3}h^2/l$. For an ellipsoid, the curvature is given by Eq. (25), which gives

$$\nabla K = -\frac{4a}{b^4}e^2(1 - e^2 \sin^2 \phi)^{5/2} \cos \phi \sin \phi; \quad (95)$$

the direction of ∇K is along the meridian towards the equator. Bounding h over all the geodesics whose end-points lie within a distance r of the center of projection, gives (in the limit that e and r are small)

$$|h| \leq \frac{f}{8} \frac{r^3}{a^3} r. \quad (96)$$

The limiting value is attained when the center of projection is at $\phi = \pm 45^\circ$ and the geodesic is running in an east-west direction with the end points at bearings $\pm 45^\circ$ or $\pm 135^\circ$ from the center.

Bowring (1997) and Williams (1997) have proposed an alternate ellipsoidal generalization of the gnomonic projection as a central projection of the ellipsoid onto a tangent plane. In

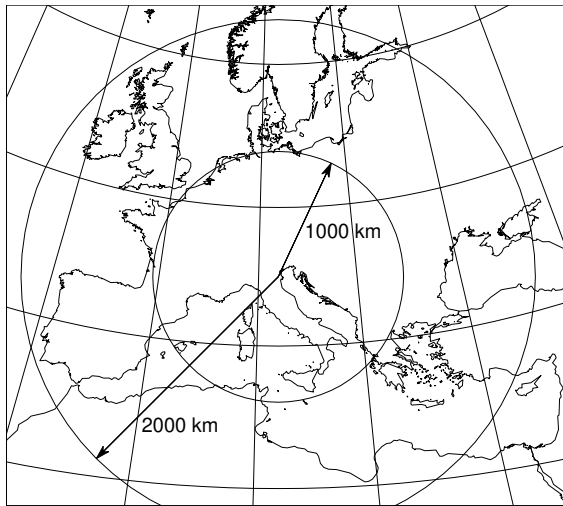


FIG. 13 The coast line of Europe and North Africa in the ellipsoidal gnomonic projection with center at (45°N, 12°E) near Venice. The graticule lines are shown at multiples of 10°. The two circles are centered on the projection center with (geodesic) radii of 1000 km and 2000 km. The data for the coast lines is taken from GMT (Wessel and Smith, 2010) at “low” resolution.

such a mapping, great ellipses project to straight lines. Empirically, I find that the deviation between straight lines in this mapping and geodesics is

$$|h| \leq \frac{f}{2} \frac{r}{a}.$$

Letoval'tsev (1963) suggested another gnomonic projection in which normal sections through the center point map to straight lines. The corresponding deviation for geodesics is

$$|h| \leq \frac{3f}{8} \frac{r^2}{a^2} r,$$

which gives a more accurate approximation to geodesics than great ellipses. However, the new definition of the spheroidal gnomonic projection, Eq. (93), results in an even smaller error, Eq. (96), in estimating geodesics. As an illustration, consider Fig. 13 in which a gnomonic projection of Europe is shown. The two circles are geodesic circles of radii 1000 km and 2000 km. If the geodesic between two points within one of these circles is estimated by using a straight line on this figure, the maximum deviation from the true geodesic will be about 1.7 m and 28 m, respectively. The maximum changes in the end azimuths are 1.1" and 8.6" and the maximum errors in the lengths are only 5.4 μm and 730 μm .

At one time, the gnomonic projection was useful for determining geodesics graphically. However, the ability to determine geodesics paths computationally renders such use of the projection an anachronism. Nevertheless, the projection can be used within an algorithm to solve some triangulation problems. For example, consider a variant of the triangulation problem 2 of Sect. 11: determine the point of intersection of two geodesics between A and B and between C and D .

This can be solved using the ellipsoidal gnomonic projection as follows. Guess an intersection point $O^{(0)}$ and use this as the center of the gnomonic projection; define \mathbf{a} , \mathbf{b} , \mathbf{c} , \mathbf{d} as the positions of A , B , C , D in the gnomonic projection; find the intersection of AB and CD in this projection, i.e.,

$$\mathbf{o} = \frac{(\hat{\mathbf{z}} \cdot \mathbf{c} \times \mathbf{d})(\mathbf{b} - \mathbf{a}) - (\hat{\mathbf{z}} \cdot \mathbf{a} \times \mathbf{b})(\mathbf{d} - \mathbf{c})}{\hat{\mathbf{z}} \cdot (\mathbf{b} - \mathbf{a}) \times (\mathbf{d} - \mathbf{c})},$$

where $\hat{\mathbf{z}}$ indicates a unit vector ($\hat{\mathbf{a}} = \mathbf{a}/a$) and $\hat{\mathbf{z}} = \hat{\mathbf{x}} \times \hat{\mathbf{y}}$ is in the direction perpendicular to the projection plane. Project \mathbf{o} back to geographic coordinates $O^{(1)}$ and use this as a new center of projection; iterate this process until $O^{(i)} = O^{(i-1)}$ which is then the desired intersection point. This algorithm converges to the exact intersection point because the mapping projects all geodesics through the center point into straight lines. The convergence is rapid because projected geodesics which pass near the center point are very nearly straight. Problem 5 of Sect. 11 can be solved using the gnomonic projection in a similar manner. If the point O on AB which is closest to C is to be found, the problem in the gnomonic space becomes

$$\mathbf{o} = \frac{\mathbf{c} \cdot (\mathbf{b} - \mathbf{a})(\mathbf{b} - \mathbf{a}) - (\hat{\mathbf{z}} \cdot \mathbf{a} \times \mathbf{b})\hat{\mathbf{z}} \times (\mathbf{b} - \mathbf{a})}{|\mathbf{b} - \mathbf{a}|^2};$$

in this case, the method relies on the preservation of azimuths about the center point.

Another application of the gnomonic projection is in solving for region intersections, unions, etc. For example the intersection of two polygons can be determined by projecting the polygons to planar polygons with the gnomonic projection about some suitable center. Any place where the edges of the polygons intersect *or nearly intersect* in the projected space is a candidate for an intersection on the ellipsoid which can be found exactly using the techniques given above. The inequality (96) can be used to define how close to intersection the edges must be in projection space to be candidates for intersection on the ellipsoid.

The methods described here suffer from the drawback that the gnomonic projection can be used to project only about one half of the ellipsoid about a given center. This is unlikely to be a serious limitation in practice and can, of course, be eliminated by partitioning a problem covering a large area into a few smaller sub-problems.

14. MARITIME BOUNDARIES

Maritime boundaries are defined to be a fixed distance from the coast of a state or, in the case of adjacent states or opposite states, as the “median line” between the states (TALOS, 2006, Chaps. 5–6). In the application of these rules, distances are defined as the geodesic distance on a reference ellipsoid to the nearest point of a state and the extent of a state is defined either by points on the low water mark or straight lines closing off bays or joining islands to the mainland.

For median lines, several cases can then be enumerated (TALOS, 2006, Chap. 6): the median is determined by two

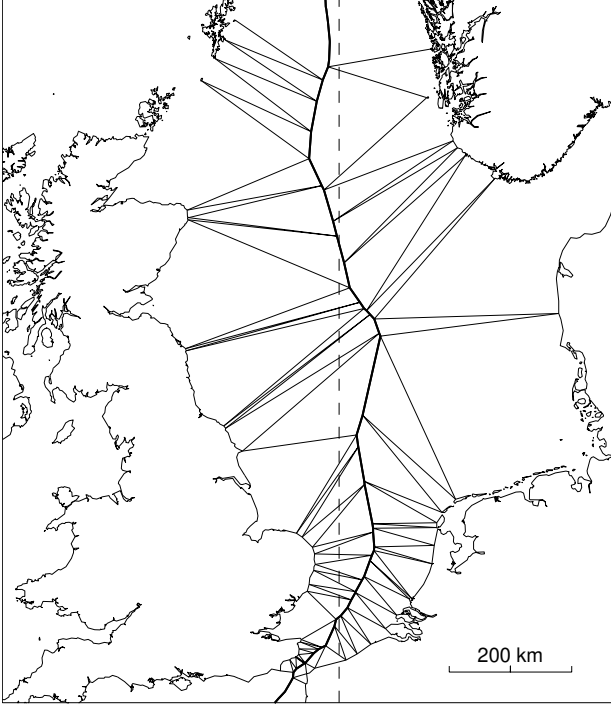


FIG. 14 The median line (shown as a heavy line) between Britain and her North Sea neighbors. Light lines connect the median line to the controlling boundary points. The Cassini-Soldner projection is used with the central meridian (shown as a dashed line) equal to $2^{\circ}20'15''\text{E}$ (the longitude of Paris). The data for the coast lines is taken from GMT (Wessel and Smith, 2010) at “intermediate” resolution.

points, a point and a line, or two lines. In the first case, the boundary is analogous to the perpendicular bisector in plane geometry. It may be constructed by determining the midpoint of the geodesic joining the two points and then marking off successive points either side of the geodesic by solving the 2-distance triangulation problem (problem 1 in Sect. 11) using increasing distances. This continues until some other coastal point becomes closer, at which point the median line changes direction and continues as the perpendicular bisector of a new pair of points. Such turning points are called “tri-points” and are equidistant from two points of one state and two point of the other; such a point is the center of the geodesic circle circumscribing the triangle formed by the three points.

I consider first the problem of determining a tri-point O given the three coastal points A , B , and C . The solution is an iterative one which is conveniently described in terms of the azimuthal equidistant projection. Make an initial guess $O^{(0)}$ for the position of the tri-point. Map A , B , and C to the azimuthal equidistant projection with $O^{(0)}$ as the center and denote their positions in this projection as \mathbf{a} , \mathbf{b} , and \mathbf{c} . Compute the center \mathbf{o} of the circle circumscribing the triangle formed by these three points,

$$\mathbf{o} = \frac{(a^2(\mathbf{b} - \mathbf{c}) + b^2(\mathbf{c} - \mathbf{a}) + c^2(\mathbf{a} - \mathbf{b})) \times \hat{\mathbf{z}}}{2(\mathbf{a} - \mathbf{b}) \times (\mathbf{b} - \mathbf{c}) \cdot \hat{\mathbf{z}}}. \quad (97)$$

Project \mathbf{o} to geographic coordinates $O^{(1)}$ and use this as the new center of projection. Repeat these steps until convergence. This process converges to the required tri-point because of the equidistant property of the projection and it converges rapidly because of the projection is azimuthal. If the points are sufficiently distant (in other words if the center of the projection is sufficiently close to the tri-point), Eq. (97) can be replaced by

$$\mathbf{o} = - \frac{((a - b)\hat{\mathbf{c}} + (b - c)\hat{\mathbf{a}} + (c - a)\hat{\mathbf{b}}) \times \hat{\mathbf{z}}}{(\hat{\mathbf{a}} - \hat{\mathbf{b}}) \times (\hat{\mathbf{b}} - \hat{\mathbf{c}}) \cdot \hat{\mathbf{z}}}. \quad (98)$$

Figure 14 shows the result of using this method to determine the median line separating Britain and her North Sea neighbors.

With slight modifications this procedure can be applied if any of the coast points are replaced by lines. For example, assume that A is replaced by a line and let A now denote the point on the line closest to O . At the same time as picking $O^{(0)}$, provide an estimate $A^{(0)}$ for the position of A . (These can be the result of solving problem 5 of Sect. 11; however, it’s more efficient to interleave this solution with the iteration for the tri-point.) Transform $A^{(0)}$, B , and C to the azimuthal projection and obtain $O^{(1)}$ using either Eq. (97) or (98). Also update the estimates for A to $A^{(1)}$ using one step of Newton’s method with Eq. (89). In this update, use the computed angle between the line and the geodesic from $O^{(0)}$ to $A^{(0)}$ corrected for the anticipated change due to \mathbf{o} ; this is $\mathbf{o} \times \hat{\mathbf{a}} \cdot \hat{\mathbf{z}}$ divided by the reduced length of the geodesic from $O^{(0)}$ to $A^{(0)}$. Repeat these steps until convergence.

The median line between two points A and B (or lines) can be found similarly. In this case, introduce a third point C (or line), use the distance to C as a control variable, and determine the point which is equidistant from A and B and a distance c_0 from C . By adjusting c_0 a set of regularly spaced points along the median line can be found. The algorithm is similar to the solving for the tri-point using Eq. (98); however, the updated position of the median point in the projected space is

$$\mathbf{o} = - \frac{((c - c_0)(\hat{\mathbf{a}} - \hat{\mathbf{b}}) - (a - b)\hat{\mathbf{c}}) \times \hat{\mathbf{z}}}{(\hat{\mathbf{a}} - \hat{\mathbf{b}}) \times \hat{\mathbf{c}} \cdot \hat{\mathbf{z}}}. \quad (99)$$

Boundaries which are a fixed distance from a state, typically 12NM for territorial seas or 200NM for exclusive economic zones, can be found using the same machinery (TALOS, 2006, Chap. 5). If the coast is defined by a set of points, the boundary is a set of circular arcs which meet at points which are equidistant from two coastal points. The general problem is to determine the point with is a distance a_0 from A and b_0 from B ; A is a coast point or a point on a coastal line and $a_0 = 12\text{NM}$; B is another such point when determining where two circular arcs meet in which case $b_0 = a_0$, or is a control point in which case b_0 measures off the distance along a circular arc. This is just problem 1 of Sect. 11; however, it can also be solving using the azimuthal equidistant projection in a similar manner to finding the median line. The formula for updating the boundary point in this

case is

$$\mathbf{o} = \frac{((a - a_0)\hat{\mathbf{b}} - (b - b_0)\hat{\mathbf{a}}) \times \hat{\mathbf{z}}}{\hat{\mathbf{a}} \times \hat{\mathbf{b}} \cdot \hat{\mathbf{z}}}. \quad (100)$$

Figure 14 was obtained by exhaustively computing the distances to all the coastal points at each point along the median line. This is reasonably fast for small data sets, $N \lesssim 1000$ points. For larger data sets, the points should be organized in such a way that the distance to the closest point can be computed quickly. For example, the points can be organized into quad trees (Finkel and Bentley, 1974) where every node in the tree can be characterized by a center and a radius r . The geodesic triangle inequality can be used to give bounds on the distance s from a point P to any point within the node in terms of the distance s_0 to its center, namely $\max(0, s_0 - r) \leq s \leq s_0 + r$. Once the quad tree has been constructed, which takes $O(N \log N)$ operations, computing the closest distance takes only $O(\log N)$ operations.

15. AREAS OF A GEODESIC POLYGON

The last geodesic problem I consider is the computation of the area of a geodesic polygon. Here, I extend the method of Danielsen (1989) to higher order so that the result is accurate to round-off, and I recast his series into a simple trigonometric sum which is amenable to Clenshaw summation. In formulating the problem, I follow Sjöberg (2006).

The area of an arbitrary region on the ellipsoid is given by

$$T = \int dT, \quad (101)$$

where $dT = \cos \phi d\phi d\lambda / K$ is an element of area and K is the Gaussian curvature. Compare this with the Gauss–Bonnet theorem (Eisenhart, 1940, §34) (Bonnet, 1848, §105)

$$\Gamma = \int K dT, \quad (102)$$

where $\Gamma = 2\pi - \sum_j \theta_j$ is the geodesic excess. This form of the theorem applies only for a polygon whose sides are geodesics and the sum is over its vertices and θ_j is the exterior angle at vertex j . Sjöberg combines Eqs. (101) and (102) to give

$$\begin{aligned} T &= c^2 \Gamma + \int \left(\frac{1}{K} - c^2 \right) \cos \phi d\phi d\lambda \\ &= c^2 \Gamma + \int \left(\frac{b^2}{(1 - e^2 \sin^2 \phi)^2} - c^2 \right) \cos \phi d\phi d\lambda, \end{aligned} \quad (103)$$

where c is a constant, and K has been evaluated using Eqs. (7) and (25). Now apply Eq. (103) to the geodesic quadrilateral $AFHB$ in Fig. 1 for which $\Gamma = \alpha_2 - \alpha_1$ and the integration over ϕ may be performed to give

$$\begin{aligned} S_{12} &= c^2(\alpha_2 - \alpha_1) + b^2 \int_{\lambda_1}^{\lambda_2} \left(\frac{1}{2(1 - e^2 \sin^2 \phi)} \right. \\ &\quad \left. + \frac{\tanh^{-1}(e \sin \phi)}{2e \sin \phi} - \frac{c^2}{b^2} \right) \sin \phi d\lambda, \end{aligned} \quad (104)$$

where S_{12} is the area of the geodesic quadrilateral and integral is over the geodesic line (so that ϕ is implicitly a function of λ). Convert this to an integral over the spherical arc length σ using a similar technique to that used in deriving Eq. (23). Sjöberg chooses $c = b$; however, this leads to a singular integrand when the geodesics pass over a pole. (In addition, he expresses the integral in terms of the latitude which leads to greater errors in its numerical evaluation.) In contrast, I define

$$c^2 = R_q^2 = \frac{a^2}{2} + \frac{b^2 \tanh^{-1} e}{2e}, \quad (105)$$

which is, in effect, the choice that Danielsen makes and which leads to a non-singular integrand. The quantity R_q is the authalic radius, the radius of the sphere with the same area as the ellipsoid. Expressing S_{12} in terms of σ gives

$$S_{12} = S(\sigma_2) - S(\sigma_1), \quad (106)$$

$$S(\sigma) = R_q^2 \alpha + e^2 a^2 \cos \alpha_0 \sin \alpha_0 I_4(\sigma), \quad (107)$$

where

$$I_4(\sigma) = - \int_{\pi/2}^{\sigma} \frac{t(e'^2) - t(k^2 \sin^2 \sigma')}{e'^2 - k^2 \sin^2 \sigma'} \frac{\sin \sigma'}{2} d\sigma', \quad (108)$$

and

$$t(x) = x + \sqrt{x^{-1} + 1} \sinh^{-1} \sqrt{x}, \quad (109)$$

and I have chosen the limits of integration in Eq. (108) so that the mean value of the integral vanishes. Expanding the integrand in powers of k^2 and e'^2 (the same expansion parameters as Danielsen uses) and performing the integral gives

$$I_4(\sigma) = \sum_{l=0}^{\infty} C_{4l} \cos((2l+1)\sigma), \quad (110)$$

where

$$\begin{aligned} C_{40} &= \left(\frac{2}{3} - \frac{1}{15}e'^2 + \frac{4}{105}e'^4 - \frac{8}{315}e'^6 + \frac{64}{3465}e'^8 - \frac{128}{9009}e'^{10} \right) \\ &\quad - \left(\frac{1}{20} - \frac{1}{35}e'^2 + \frac{2}{105}e'^4 - \frac{16}{1155}e'^6 + \frac{32}{3003}e'^8 \right) k^2 \\ &\quad + \left(\frac{1}{42} - \frac{1}{63}e'^2 + \frac{8}{693}e'^4 - \frac{80}{9009}e'^6 \right) k^4 \\ &\quad - \left(\frac{1}{72} - \frac{1}{99}e'^2 + \frac{10}{1287}e'^4 \right) k^6 \\ &\quad + \left(\frac{1}{110} - \frac{1}{143}e'^2 \right) k^8 - \frac{1}{156}k^{10} + \dots, \\ C_{41} &= \left(\frac{1}{180} - \frac{1}{315}e'^2 + \frac{2}{945}e'^4 - \frac{16}{10395}e'^6 + \frac{32}{27027}e'^8 \right) k^2 \\ &\quad - \left(\frac{1}{252} - \frac{1}{378}e'^2 + \frac{4}{2079}e'^4 - \frac{40}{27027}e'^6 \right) k^4 \\ &\quad + \left(\frac{1}{360} - \frac{1}{495}e'^2 + \frac{2}{1287}e'^4 \right) k^6 \\ &\quad - \left(\frac{1}{495} - \frac{2}{1287}e'^2 \right) k^8 + \frac{5}{3276}k^{10} + \dots, \\ C_{42} &= \left(\frac{1}{2100} - \frac{1}{3150}e'^2 + \frac{4}{17325}e'^4 - \frac{8}{45045}e'^6 \right) k^4 \\ &\quad - \left(\frac{1}{1800} - \frac{1}{2475}e'^2 + \frac{2}{6435}e'^4 \right) k^6 \\ &\quad + \left(\frac{1}{1925} - \frac{2}{5005}e'^2 \right) k^8 - \frac{1}{2184}k^{10} + \dots, \\ C_{43} &= \left(\frac{1}{17640} - \frac{1}{24255}e'^2 + \frac{2}{63063}e'^4 \right) k^6 \\ &\quad - \left(\frac{1}{10780} - \frac{1}{14014}e'^2 \right) k^8 + \frac{5}{45864}k^{10} + \dots, \\ C_{44} &= \left(\frac{1}{124740} - \frac{1}{162162}e'^2 \right) k^8 - \frac{1}{58968}k^{10} + \dots, \end{aligned}$$

$$C_{45} = \frac{1}{792792} k^{10} + \dots \quad (111)$$

I have included terms up to $O(f^5)$ so that the expression for $S(\sigma)$ is accurate to $O(f^6)$. This is consistent with the order to which the distance and longitude integrals need to be evaluated to give accuracy to the round-off limit for $f = 1/150$. In contrast the series given by Danielsen (1989) gives S accurate to $O(f^4)$. Clenshaw (1955) summation can be used to perform the (truncated) sum in Eq. (110), with

$$\sum_{l=1}^L a_l \cos\left(l - \frac{1}{2}\right)x = (b_1 - b_2) \cos \frac{1}{2}x,$$

where b_l is given by Eq. (59).

Summing Eq. (106) for each side of a polygon gives the total area of the polygon, provided it does not include a pole. If it does, then $2\pi c^2$ should be added to the result. The combined round-off and truncation error in the evaluation of $I_4(\sigma)$ is about $5 \times 10^{-3} \text{ m}^2$ for the WGS84 ellipsoid. However, the bigger source of errors is in the computation of the geodesic excess, i.e., the first term in Eq. (107); the sum of these terms gives the area of the spherical polygon and, in Appendix C, I show how to calculate this accurately. The resulting errors in the area of polygon can be estimated using the data for the errors in the azimuths given in Sect. 9. Typically, the error is approximately $a \times 15 \text{ nm} = 0.1 \text{ m}^2$ per vertex; however, it may be greater if polygon vertices are very close to a pole or if a side is nearly hemispherical. Sometimes the polygon may include many thousands of vertices, e.g., determining the area of the Japan. In this case an additional source of round-off error occurs when summing the separate contributions S_{12} from each edge; this error can be controlled by using Kahan (1965) summation.

This method of area computation requires that the sides of the polygon be geodesics. If this condition is fulfilled then the work of computing the area is proportional to the number of sides of the polygon. If the sides are some other sort of lines, then additional vertices must be inserted so that the individual sides are well approximated by geodesics. Alternatively the lines can be mapped to an equal-area projection, such as the Albers conic projection (Snyder, 1987, §14), as suggested by Gillissen (1993), and the area computed in the projected space. In either of these cases, the work of computing the area will be proportional to the perimeter of the polygon.

16. CONCLUSIONS

This paper presents solutions for the direct and inverse geodesic problems which are accurate to close to machine precision; the errors are less than 15 nm using double-precision arithmetic. The algorithm for the inverse problem always converges rapidly. The algorithms also give the reduced length and geodesic scale; these provide scale factors for geodesic projections, allow Newton's method to be used to solve various problems in ellipsoidal trigonometry, and enable instrumental errors to be propagated through geodesic calculations. I introduce an ellipsoidal generalization of the gnomonic projection in which geodesics project to approximately straight

lines. I discuss the solution of several geodesic problems involving triangulation and the determination of median lines. I simplify and extend the formulas given by Danielsen (1989) for the area of geodesic polygons to arbitrary precision. The solution of the inverse geodesic problem uses a general solution for converting from geocentric to geodetic coordinates (Appendix B).

Reviewing the list of references, it is remarkable the extent to which this paper relies on 19th century authors. Indeed my solution of the direct geodesic problems is a straightforward extension of that given by Helmert (1880) to higher order. The solution for the inverse problem relies on two relatively modest innovations, the use of Newton's method to accelerate convergence and a careful choice of the starting guess to ensure convergence; however, the necessary machinery is all available in Helmert (1880). My advances, such as they are, rely on a few 20th century innovations. The most obvious one is the availability of cheap hardware and software for flexibly carrying out numerical calculations. However, equally important for algorithm development are software packages for algebraic manipulation and arbitrary precision arithmetic, both of which are provided by Maxima (2009)—these facilities have been available in Maxima since the mid 1970s.

Computer code implementing much of this work is incorporated into GeographicLib (Karney, 2010). This includes (a) C++ implementations of the solutions for the direct and inverse geodesic problem, (b) methods for computing points along a geodesic in terms of distance or spherical arc length, (c) computation of the reduced length m_{12} , the geodesic scales M_{12} and M_{21} , and the area S_{12} , (d) implementations of the azimuthal equidistant, Cassini–Soldner, and ellipsoidal gnomonic projections (all of which return projection scales), (e) command-line utilities for solving the main geodesic problems, computing geodesic projections, and finding the area of a geodesic polygon, (f) Maxima code to generate the series $I_j(\sigma)$ extract the coefficients A_j and C_{jl} , and “write” the C++ code to evaluate the coefficients, (g) the series expansions carried out to 30th order, and (h) the geodesic test data used in Sect. 9. The web page <http://geographiclib.sf.net/geod.html> provides quick links to all these resources. In this paper, I have tried to document the geodesic algorithms in GeographicLib accurately; the source code should be consulted in case of any ambiguity.

I have been questioned on the need for nanometer accuracy when geodetic measurements are frequently only accurate to about a centimeter. I can give four possible answers. (1) Geodesic routines which are accurate to 1 mm, say, can yield satisfactory results for simple problems. However, more complicated problems typically require much greater accuracy; for example, the two-point equidistant projection may entail the solution of ill-conditioned triangles for which millimeter errors in the geodesic calculation would lead to much larger errors in the results. With accurate geodesic routines packaged as “subroutines”, the azimuthal equidistant and Cassini–Soldner projections (which are usually expressed as series with limited applicability) can be easily and accurately computed for nearly the whole earth. The need for accuracy has become more pressing with the proliferation of “ge-

ographic information systems” which allow users (who may be unaware of the pitfalls of error propagation) access to geographic data. (2) Even if millimeter errors are tolerable, it is frequently important that other properties of geodesics are well satisfied, and this is best achieved by ensuring the geodesic calculations are themselves very accurate. An example of such a property is the triangle inequality; this implies that the shortest path between a point and a geodesic intersects the geodesic at right angles and it also ensures the orthogonality of the polar graticule of the azimuthal equidistant projection. (3) Accurate routines may be just as fast as inaccurate ones. In particular, the use of Clenshaw summation means that there is little penalty to going to 6th order in the expansions in Sect. 5. On a 2.66 GHz Intel processor with the g++ compiler, version 4.4.4, solving the direct geodesic problem takes $0.88 \mu\text{s}$, while the inverse problem takes $2.62 \mu\text{s}$ (on average). Points along a geodesic can be computed at the rate of $0.37 \mu\text{s}$ (resp. $0.31 \mu\text{s}$) per point when the geodesic is parametrized by distance (resp. spherical arc length). Thus the time to perform a forward and reverse azimuthal equidistant projection (equivalent to solving the inverse and direct geodesic problems) is $3.4 \mu\text{s}$, which is only about 2 times slower than computing the transverse Mercator projection using Krüger’s series (Karney, 2011). The object code in geodesic code of GeographicLib is substantially longer than an implementation of the method of Vincenty (1975a), but, at about 30 kbytes, it is negligible compared to the available memory on most computers. (4) Finally, it is desirable that a well defined mathematical problem have an accurate and complete computational solution; paraphrasing Gauss (1903, p. 378) in a letter to Olbers (in 1827, on the ellipsoidal corrections to the distribution of the geodesic excess between the angles of a spheroidal triangle), “the dignity of science (*die Würde der Wissenschaft*)” requires it.

Acknowledgments

I would like to thank Rod Deakin and Dick Rapp for comments on a preliminary version of this paper. John Nolton kindly furnished me with a copy of Vincenty (1975b).

Appendix A: Equations for a geodesic

Here, I give a derivation of Eqs. (19) following, for the most part, the presentation of Bessel (1825). Laplace (1829, Book 1, §8) shows that the path of a geodesic on a surface is the same as the motion of a particle constrained to the surface but subject to no external forces. For a spheroid of revolution, conservation of angular momentum gives the relation found by Clairaut (1735),

$$R \sin \alpha = a \sin \alpha_0, \quad (\text{A1})$$

where R is the distance from the axis of revolution (i.e., the radius of the circle of latitude), a is the maximum radius of the body, α is the azimuth of the geodesic with respect to a meridian, and α_0 is the azimuth at the latitude of maximum radius. Because $R \leq a$, R can be written as $a \cos \beta$, where β is the

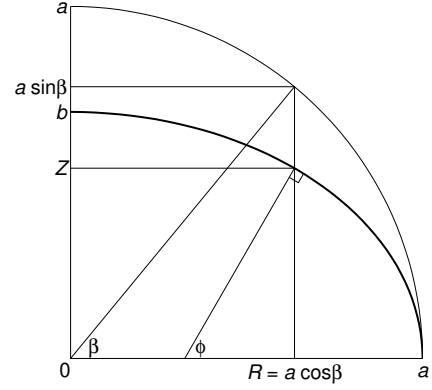


FIG. 15 The construction for the reduced latitude. The heavy curve shows a quarter meridian of the spheroid for which the latitude ϕ is defined as the angle between the normal and the equator. Points are transferred from the ellipsoid to the auxiliary sphere, shown as a light curve, by preserving the radius of the circle of latitude R . The latitude β on the auxiliary sphere is the reduced latitude defined by $R = a \cos \beta$.

latitude on the auxiliary sphere (see Fig. 15), and Eq. (A1) becomes

$$\cos \beta \sin \alpha = \sin \alpha_0. \quad (\text{A2})$$

This is the sine rule applied to the angles α_0 and $\pi - \alpha$ in the triangle NEP on the auxiliary sphere in Fig. 2 and establishes the correspondence with a geodesic on a spheroid with a great circle on the auxiliary sphere. It remains to establish the relations between λ and s and their counterparts on the sphere ω and σ . For a given geodesic on the spheroid, an elementary distance ds is related to changes in latitude and longitude by (Bessel, 1825, Eqs. (1))

$$\cos \alpha ds = \rho d\phi = -dR / \sin \phi, \quad \sin \alpha ds = R d\lambda, \quad (\text{A3})$$

where ρ is the meridional radius of curvature. The corresponding equations on the auxiliary sphere are

$$a \cos \alpha d\sigma = -dR / \sin \beta, \quad a \sin \alpha d\sigma = R d\omega. \quad (\text{A4})$$

Dividing Eqs. (A3) by Eqs. (A4) gives (Bessel, 1825, Eqs. (4))

$$\frac{1}{a} \frac{ds}{d\sigma} = \frac{d\lambda}{d\omega} = \frac{\sin \beta}{\sin \phi}. \quad (\text{A5})$$

These relations hold for geodesics on any spheroid of revolution. Specializing now to an ellipsoid of revolution, parametrically given by $R = a \cos \beta$ and $Z = b \sin \beta$. The slope of the meridian ellipse is given by

$$\frac{dZ}{dR} = -\frac{b \cos \beta}{a \sin \beta} = -\frac{\cos \phi}{\sin \phi}.$$

This gives the formula for the reduced latitude, Eq. (8), and leads to

$$\frac{\sin \beta}{\sin \phi} = \sqrt{1 - e^2 \cos^2 \beta} = w.$$

Substituting this into Eqs. (A5) gives Eqs. (19).

Appendix B: Transforming geocentric coordinates

Vermeille (2002) presented a closed-form transformation from geocentric to geodetic coordinates. However, his solution does not apply near the center of the earth. Here, I remove this restriction and improve the numerical stability of the method so that the method is valid everywhere. A key equation in Vermeille's method is the same as Eq. (65) and this method given here can therefore be used to solve this equation. While this paper was being prepared, Vermeille (2011) published an update on his earlier paper which addresses some of the same problems.

As in the main body of this paper, the earth is treated as an ellipsoid with equatorial radius a and eccentricity e . The geocentric coordinates are represented by (X, Y, Z) and the method transforms this to geodetic coordinates (λ, ϕ, h) where h is the height measured normally from the surface of the ellipsoid. Geocentric coordinates are given in terms of geographic coordinates by

$$\begin{aligned} X &= (a \cos \beta + h \cos \phi) \cos \lambda, \\ Y &= (a \cos \beta + h \cos \phi) \sin \lambda, \\ Z &= b \sin \beta + h \sin \phi, \end{aligned}$$

where $\sin \beta = w \sin \phi$, $\cos \beta = w \cos \phi / \sqrt{1 - e^2}$ and w is given by Eq. (20). In inverting these equations, the determination of λ is trivial,

$$\lambda = \text{ph}(X + iY).$$

This reduces the problem to a two-dimensional one, converting (R, Z) to (ϕ, h) where $R = \sqrt{X^2 + Y^2}$. Vermeille reduces the problem to the solution of an algebraic equation

$$\kappa^4 + 2e^2\kappa^3 - (x^2 + y^2 - e^4)\kappa^2 - 2e^2y^2\kappa - e^4y^2 = 0, \quad (\text{B1})$$

where

$$x = R/a, \quad y = \sqrt{1 - e^2}Z/a.$$

Descartes' rule of signs shows that for $y \neq 0$, Eq. (B1) has one positive root (Olver *et al.*, 2010, §1.11(ii)). Similarly for $x \neq 0$, it has one root satisfying $\kappa < -e^2$. Inside the astroid, $x^{2/3} + y^{2/3} < e^{4/3}$, there are two additional roots satisfying $-e^2 < \kappa < 0$.

The geodetic coordinates are given by substituting the real solutions for κ into

$$\phi = \text{ph}(R/(\kappa + e^2) + iZ/\kappa), \quad (\text{B2})$$

$$h = \left(1 - \frac{1 - e^2}{\kappa}\right) \sqrt{D^2 + Z^2}, \quad (\text{B3})$$

where $D = \kappa R/(\kappa + e^2)$. The positive real root gives the largest value of h and I call this the "standard solution".

Equation (B1) may be solved by standard methods (Olver *et al.*, 2010, §1.11(iii)). Here, I summarize Vermeille's solution modifying it to extend its range of validity and to im-

prove the accuracy. The solution proceeds as follows

$$\begin{aligned} r &= \frac{1}{6}(x^2 + y^2 - e^4), \\ S &= \frac{1}{4}e^4x^2y^2, \\ d &= S(S + 2r^3), \\ T &= (S + r^3 \pm \sqrt{d})^{1/3}, \\ u &= r + T + r^2/T. \end{aligned}$$

For $d \geq 0$, the sign of the square root in the expression for T should match the sign of $S + r^3$ in order to minimize round-off errors; also, the real cube root should be taken. If $T = 0$, then take $u = 0$. For $d < 0$, T is complex, and u is given by

$$\begin{aligned} \psi &= \text{ph}(-S - r^3 + i\sqrt{-d}), \\ T &= r \exp \frac{1}{3}i\psi, \\ u &= r(1 + 2 \cos \frac{1}{3}\psi). \end{aligned}$$

The right-hand side of Eq. (B1) may now be factored into 2 quadratic terms in terms of u

$$\kappa^2 + \frac{(v \pm u) \mp y^2}{v} e^2 \kappa \mp (v \pm u), \quad (\text{B4})$$

where

$$\begin{aligned} v &= \sqrt{u^2 + e^4y^2}, \\ v \pm u &= \frac{e^4y^2}{v \mp u}, \quad \text{for } u \leq 0, \end{aligned}$$

and where the latter equation merely gives a way to avoid round-off error in the computation of $v \pm u$. Only the factor with the upper signs in Eq. (B4) has a positive root given by

$$\kappa = \frac{v + u}{\sqrt{(v + u) + w^2} + w}, \quad (\text{B5})$$

where

$$w = \frac{(v + u) - y^2}{2v} e^2.$$

The number of real roots of Eq. (B1) is determined as follows. The condition $d \geq 0$ is equivalent to $x^{2/3} + y^{2/3} \geq e^{4/3}$. For $d > 0$, only the quadratic factor with the upper signs in Eq. (B4) has real roots (satisfying $\kappa > 0$ and $\kappa < -e^2$, respectively). For $d < 0$, both factors have real roots yielding the four real roots of Eq. (B1).

Equations (B2) and (B3) may become ill-defined if x or y vanishes. Solving Eq. (B1) in the limit $x \rightarrow 0$ gives

$$\kappa = \pm y, \quad \kappa = -e^2 \pm e^2x/\sqrt{e^4 - y^2}. \quad (\text{B6})$$

Similarly in the limit $y \rightarrow 0$, Eq. (B1) yields

$$\kappa = -e^2 \pm x, \quad \kappa = \pm e^2y/\sqrt{e^4 - x^2}. \quad (\text{B7})$$

The only case where these limiting forms are needed in determining the standard solution are for $y = 0$ and $x \leq e^2$.

Substituting the roots given by the second equation (B7) into Eqs. (B2) and (B3) gives

$$\begin{aligned}\phi &= \text{ph}(\sqrt{1 - e^2 x \pm i\sqrt{e^4 - x^2}}), \\ h &= -b\sqrt{1 - x^2/e^2}.\end{aligned}$$

In the solution given here, I assumed that the ellipsoid is oblate. This solution encompasses also the spherical limit, $e \rightarrow 0$; the solution becomes $\kappa^2 \rightarrow x^2 + y^2$. The method may also be applied to a prolate ellipsoid, $e^2 < 0$. Substituting $x = y'$, $y = x'$, $\kappa = \kappa' - e^2$ in Eq. (B1) gives

$$\kappa'^4 - 2e^2\kappa'^3 - (x'^2 + y'^2 - e^4)\kappa'^2 + 2e^2y'^2\kappa' - e^4y'^2 = 0,$$

which transforms the problem for a prolate ellipsoid into an equivalent problem for an oblate one.

In applying the results of this appendix to the inverse geodesic problem, set $e = 1$ in order to convert Eq. (B1) into Eq. (65).

Appendix C: Area of a spherical polygon

The area S_{12} , Eq. (104), includes the term $c^2(\alpha_2 - \alpha_1)$. Round-off errors in the evaluation of this term is a potential source of error in determining S_{12} . In this appendix, I investigate ways to compute this term accurately. This term

$$E_{12} = \alpha_2 - \alpha_1 \quad (\text{C1})$$

is of course merely the spherical excess for the quadrilateral $AFGB$ in Fig. 1 transferred to the auxiliary sphere. Thus E_{12} is the spherical excess for the quadrilateral with vertices (β_1, ω_1) , $(0, \omega_1)$, $(0, \omega_2)$, and (β_2, ω_2) .

If the geodesic AB is determined by its arc length σ_{12} and its azimuth α_1 at A then use Eq. (12) to determine α_2 and so write

$$\tan E_{12} = \frac{\sin \alpha_0 \cos \alpha_0 (\cos \sigma_1 - \cos \sigma_2)}{\sin^2 \alpha_0 + \cos^2 \alpha_0 \cos \sigma_1 \cos \sigma_2}, \quad (\text{C2})$$

with

$$\begin{aligned}\cos \sigma_1 - \cos \sigma_2 &= \\ \left\{ \begin{array}{ll} \sin \sigma_{12} \left(\frac{\cos \sigma_1 \sin \sigma_{12}}{1 + \cos \sigma_{12}} + \sin \sigma_1 \right), & \text{if } \cos \sigma_{12} > 0, \\ \cos \sigma_1 (1 - \cos \sigma_{12}) + \sin \sigma_{12} \sin \sigma_1, & \text{otherwise.} \end{array} \right.\end{aligned}$$

Here, α_0 and σ_1 can be determined as described in Sect. 6.

If the geodesic AB is determined by the latitude and longitude of its end points, then, for long arcs, determine α_1 and α_2 from Eqs. (68) and (69), and substitute these values into Eq. (C1). If, on the other hand, the arc is short, use

$$\tan \frac{E_{12}}{2} = \frac{\tan \frac{1}{2}\beta_1 + \tan \frac{1}{2}\beta_2}{1 + \tan \frac{1}{2}\beta_1 \tan \frac{1}{2}\beta_2} \tan \frac{\omega_{12}}{2}, \quad (\text{C3})$$

where, if $\sin \theta$ and $\cos \theta$ are already known, $\tan \frac{1}{2}\theta$ may be evaluated as $\sin \theta / (1 + \cos \theta)$. This relation is the spherical

generalization of the trapezoidal area; in the limit $\beta_1 \rightarrow 0$, $\beta_2 \rightarrow 0$, $\omega_{12} \rightarrow 0$, Eq. (C3) becomes

$$E_{12} \rightarrow \frac{\beta_1 + \beta_2}{2} \omega_{12}.$$

Equation (C3) takes on a simpler form if the latitude is expressed in terms of the so-called isometric latitude, $\psi = 2 \tanh^{-1} \tan \frac{1}{2}\beta = \sinh^{-1} \tan \beta$, namely

$$\tan \frac{E_{12}}{2} = \tanh \frac{\psi_1 + \psi_2}{2} \tan \frac{\omega_{12}}{2}.$$

I obtained Eq. (C3) from the formula for the area of a spherical triangle, E , in terms of two of the sides, a and b , and their included angle γ (Todhunter, 1871, §103),

$$\tan \frac{E}{2} = \frac{\tan \frac{1}{2}a \tan \frac{1}{2}b \sin \gamma}{1 + \tan \frac{1}{2}a \tan \frac{1}{2}b \cos \gamma},$$

by substituting $a = \frac{1}{2}\pi + \beta_1$, $b = \frac{1}{2}\pi + \beta_2$, $\gamma = \omega_{12}$, and forming $E_{12} = E - \omega_{12}$. However, it can also be simply found by using a formula of Bessel (1825, §11),

$$\tan \frac{\alpha_2 - \alpha_1}{2} = \frac{\sin \frac{1}{2}(\beta_2 + \beta_1)}{\cos \frac{1}{2}(\beta_2 - \beta_1)} \tan \frac{\omega_{12}}{2},$$

which, in turn, is derived from one of Napier's analogies (Todhunter, 1871, §52).

The area for an N -sided spherical polygon is obtained by

$$2\pi n - \sum_{i=1}^N E_{i-1,i},$$

where n is the number of times the polygon encircles the sphere in the easterly direction.

Miller (1994) proposed a formula for the area of a spherical polygon which made use of L'Huilier's theorem for the area of a spherical triangle in terms of its three sides (Todhunter, 1871, §102). However, any edge of the polygon which is nearly aligned with a meridian leads to an ill-conditioned triangle which results in about half of the precision of the floating-point numbers being lost.

Appendix D: Geodesics on a prolate ellipsoid

The focus in the paper has been on oblate ellipsoids. However, most of the analysis applies also to prolate ellipsoids ($f < 0$). In the appendix, I detail those aspects of the problem which need to be treated differently in the two cases.

All the series expansions given in Sect. 5 and the expansions for S_{12} given in Sect. 15 are in terms of f , n , e^2 or e'^2 ; prolate ellipsoids may be treated easily by allowing these quantities to become negative. The method of solving the direct geodesic problem requires no alteration. The solution of inverse problem, on the other hand, is slightly different. From Eq. (23), it can be seen that the longitude difference for a geodesic encircling the auxiliary sphere exceeds 2π . As a consequence, the shortest geodesic between any two points on

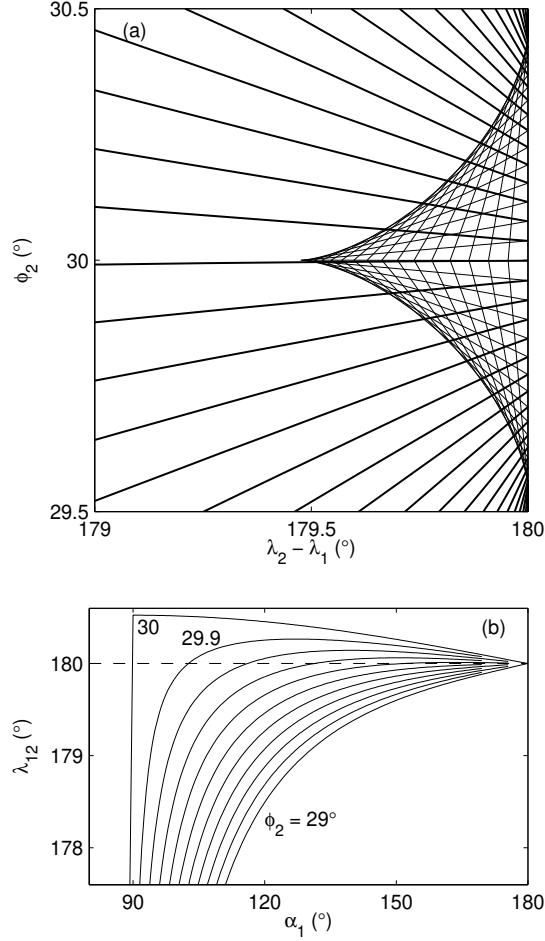


FIG. 16 (a) Geodesics in antipodal region for a prolate ellipsoid. This figure is similar to Fig. 4a, except that $f = -1/297$. In addition the light lines are the continuation of the symmetric set of west-going geodesics beyond the meridian $\lambda_{12} = 180^\circ$. (b) The dependence of λ_{12} on α_1 for the near antipodal case with the same value of the flattening; compare with Fig. 7b.

the equator is equatorial; however, the shortest geodesics between two points on the same meridian may not run along the meridian if the points are nearly antipodal. The test for meridional geodesics needs therefore to include the requirement $m_{12} \geq 0$. The solution for the inverse geodesic problem is also unchanged except that the method of choosing starting points for Newton's method needs to be altered in case 3 in Fig. 9. The envelope of the geodesics forms an astroid, Fig. 16a, however, the x and y axes need to be interchanged to match Fig. 4a, and with this substitution, the derivation of the starting point depicted in Fig. 5 applies. Similarly region 3b in Fig. 9, now lies along the meridian $\lambda_{12} = \pi$. The techniques for solving the antipodal problem for a prolate ellipsoid mirror closely those needed to transform geocentric coordinates as described at the end of Appendix B. The longitude difference λ_{12} as a function of α_1 is no longer monotonic when the ellipsoid is prolate; see Fig. 16b. This potentially complicates the determination of α_1 ; nevertheless, the starting points used in

region 3 are sufficiently accurate that Newton's method converges. The geodesic classes in GeographicLib handle prolate ellipsoids; however, the algorithms have not been thoroughly tested with geodesics on prolate ellipsoids.

Some of the closed form expressions can be recast into real terms for prolate ellipsoids. Thus Eqs. (36)–(41) should be replaced by

$$I_1(\sigma) = \int_0^{u_2} \operatorname{dn}^2(u', k_2) du' = E(\sigma, k_2), \quad (\text{D1})$$

$$I_2(\sigma) = u_2 = F(\sigma, k_2), \quad (\text{D2})$$

$$\begin{aligned} I_3(\sigma) &= -\frac{1-f}{f} \int_0^{u_2} \frac{\operatorname{dn}^2(u', k_2)}{1 - \cos^2 \alpha_0 \operatorname{sn}^2(u', k_2)} du' \\ &\quad + \frac{\tan^{-1}(\sin \alpha_0 \tan \sigma)}{f \sin \alpha_0} \\ &= -\frac{1-f}{f} G(\sigma, \cos^2 \alpha_0, k_2) \\ &\quad + \frac{\tan^{-1}(\sin \alpha_0 \tan \sigma)}{f \sin \alpha_0}, \end{aligned} \quad (\text{D3})$$

where $k_2 = \sqrt{-k^2}$,

$$\operatorname{am}(u_2, k_2) = \sigma,$$

$\operatorname{sn}(x, k)$ and $\operatorname{dn}(x, k)$ are Jacobian elliptic functions (Olver *et al.*, 2010, §22.2), and $G(\phi, \alpha^2, k)$ is defined by Eq. (42), as before. In this form, the integration constants vanish. Finally, Eq. (105) becomes

$$c^2 = \frac{a^2}{2} + \frac{b^2 \tan^{-1} \sqrt{-e^2}}{2 \sqrt{-e^2}}, \quad (\text{D4})$$

and Eq. (109), which appears in the integral for the geodesic area, should be replaced by

$$t(-y) = -y + \sqrt{y^{-1} - 1} \sin^{-1} \sqrt{y}. \quad (\text{D5})$$

References

- G. V. Bagratuni, 1967, *Course in spheroidal geodesy*, Technical Report FTD-MT-64-390, US Air Force, translation of *Kurs sferoidicheskoi geodezii* (Geodezizdat, Moscow, 1962), by Foreign Technology Division, Wright-Patterson AFB, <http://handle.dtic.mil/100.2/AD650520>.
- E. Beltrami, 1865, *Risoluzione del problema: Riportare i punti di una superficie sopra un piano in modo che le linee geodetiche vengano rappresentate da linee rette*, *Annali Mat. Pura App.*, **7**, 185–204, <http://books.google.com/books?id=dfgEAAAAYAAJ&pg=PA185>.
- F. W. Bessel, 1825, *Über die Berechnung der geographischen Längen und Breiten aus geodätischen Vermessungen*, *Astron. Nachr.*, **4**(86), 241–254, doi:10.1002/asna.201011352, translated into English by C. F. F. Karney and R. E. Deakin as *The calculation of longitude and latitude from geodesic measurements*, *Astron. Nachr.* **331**(8), 852–861 (2010), E-print arXiv:0908.1824, <http://adsabs.harvard.edu/abs/1825AN.....4..241B>.
- P. O. Bonnet, 1848, *Mémoire sur la théorie générale des surfaces*, J. l'École Polytechnique, **19**(32), 1–146, http://books.google.com/books?id=VGo_AAAAcAAJ&pg=PA1.

- B. R. Bowring, 1996, *Total inverse solutions of the geodesic and great elliptic*, Survey Review, **33**(261), 461–476.
- , 1997, *The central projection of the spheroid and surface lines*, Survey Review, **34**(265), 163–173.
- L. M. Bugayevskiy and J. P. Snyder, 1995, *Map Projections: A Reference Manual* (Taylor & Francis, London), <http://www.worldcat.org/oclc/31737484>.
- R. Bulirsch, 1965, *Numerical calculation of elliptic integrals and elliptic functions*, Num. Math., **7**(1), 78–90, doi:10.1007/BF01397975.
- B. C. Carlson, 1995, *Numerical computation of real or complex elliptic integrals*, Numerical Algorithms, **10**(1), 13–26, doi:10.1007/BF02198293, E-print arXiv:math/9409227.
- A. Cayley, 1870, *On the geodesic lines on an oblate spheroid*, Phil. Mag. (4th ser.), **40**(268), 329–340, <http://books.google.com/books?id=Zk0wAAAAIAAJ&pg=PA329>.
- E. B. Christoffel, 1910, *Allgemeine Theorie der geodätischen Dreiecke (1868)*, in L. Maurer, editor, *Gesammelte Mathematische Abhandlungen*, volume 1, chapter 16, pp. 297–346 (Teubner, Leipzig), reprint of Math. Abhand. König. Akad. der Wiss. zu Berlin **8**, 119–176 (1868), <http://books.google.com/books?id=9W9tAAAAIAAJ&pg=PA297>.
- A. C. Clairaut, 1735, *Détermination géométrique de la perpendiculaire à la méridienne tracée par M. Cassini*, Mém. de l'Acad. Roy. des Sciences de Paris 1733, pp. 406–416, <http://books.google.com/books?id=GOAEAAAQAAJ&pg=PA406>.
- C. W. Clenshaw, 1955, *A note on the summation of Chebyshev series*, Math. Tables Aids Comput., **9**(51), 118–120, <http://www.jstor.org/stable/2002068>.
- J. F. Cox, 1946, *The double equidistant projection*, Bull. Géod., **2**(1), 74–76, doi:10.1007/BF02521618.
- , 1951, *La projection équidistante pour deux points*, Bull. Géod., **19**(1), 57–60, doi:10.1007/BF02527404.
- J. Danielsen, 1989, *The area under the geodesic*, Survey Review, **30**(232), 61–66.
- J. G. Darboux, 1894, *Leçons sur la Théorie Générale des Surfaces*, volume 3 (Gauthier-Villars, Paris), <http://books.google.com/books?id=hGMSAAAIAAJ>.
- A. P. Dionis du Séjour, 1789, *Traité Analytique des Mouvements apparens des Corps Célestes*, volume 2 (Valade, Paris), <http://books.google.com/books?id=tnHOAAAIAAJ>.
- L. P. Eisenhart, 1909, *A Treatise on the Differential Geometry of Curves and Surfaces* (Ginn & Co., Boston), <http://books.google.com/books?id=hkENAAAIAAJ>.
- , 1940, *An Introduction to Differential Geometry* (Princeton Univ. Press), <http://www.worldcat.org/oclc/3165048>.
- L. Euler, 1755, *Éléments de la trigonométrie sphéroïdique tirés de la méthode des plus grands et plus petits*, Mém. de l'Acad. Roy. des Sciences de Berlin, **9**, 258–293, <http://books.google.com/books?id=QIIfAAAIAAJ&pg=PA258>.
- R. A. Finkel and J. L. Bentley, 1974, *Quad Trees, a data structure for retrieval on composite keys*, Acta Informatica, **4**(1), 1–9, doi:10.1007/BF00288933.
- A. R. Forsyth, 1896, *Geodesics on an oblate spheroid*, Mess. Math., **25**, 81–124, <http://books.google.com/books?id=YsAKAAAIAAJ&pg=PA81>.
- C. F. Gauss, 1902, *General Investigations of Curved Surfaces of 1827 and 1825* (Princeton Univ. Lib.), translation of *Disquisitiones generales circa superficies curvas*, by J. C. Morehead and A. M. Hildebeitel, <http://books.google.com/books?id=a1wTJR3kHwUC>.
- , 1903, *Werke*, volume 9 (Teubner, Leipzig), <http://books.google.com/books?id=ICwPAAAIAAJ>.
- I. Gillissen, 1993, *Area computation of a polygon on an ellipsoid*, Survey Review, **32**(248), 92–98.
- F. R. Helmert, 1880, *Die Mathematischen und Physikalischen Theorien der Höheren Geodäsie*, volume 1 (Teubner, Leipzig), translated into English by Aeronautical Chart and Information Center (St. Louis, 1964) as *Mathematical and Physical Theories of Higher Geodesy, Part 1* (<http://geographiclib.sf.net/geodesic-papers/helmert80-en.html>), <http://books.google.com/books?id=qt2CAAAAIAAJ>.
- D. Hilbert and S. Cohn-Vossen, 1952, *Geometry and the Imagination* (Chelsea, New York), translation of *Anschauliche Geometrie* (1932), by P. Nemenyi, <http://www.worldcat.org/oclc/301610346>.
- A. R. Hinks, 1929, *A retro-azimuthal equidistant projection of the whole sphere*, Geog. J., **73**(3), 245–247, <http://www.jstor.org/stable/1784715>.
- C. G. J. Jacobi, 1855, *Solution nouvelle d'un problème de géodésie fondamentale*, Astron. Nachr., **41**(974), 209–216, doi:10.1002/asna.18550411401, op. post., communicated by E. Luther, <http://adsabs.harvard.edu/abs/1855AN.....41..209J>.
- , 1891, *Über die Curve, welche alle von einem Punkte ausgehenden geodätischen Linien eines Rotationsellipsoides berührt*, in K. T. W. Weierstrass, editor, *Gesammelte Werke*, volume 7, pp. 72–87 (Reimer, Berlin), op. post., completed by A. Wangerin, <http://books.google.com/books?id=.09tAAAAIAAJ&pg=PA72>.
- W. M. Kahan, 1965, *Further remarks on reducing truncation errors*, Comm. ACM, **8**(1), 40, doi:10.1145/363707.363723.
- C. F. F. Karney, 2009, *An online geodesic bibliography*, <http://geographiclib.sf.net/geodesic-papers/biblio.html>.
- , 2010, *GeographicLib, version 1.7*, <http://geographiclib.sf.net>.
- , 2011, *Transverse Mercator with an accuracy of a few nanometers*, J. Geod., doi:10.1007/s00190-011-0445-3, in press, E-print arXiv:1002.1417.
- J. L. Lagrange, 1869, *Nouvelle méthode pour résoudre les équations littérales par le moyen des séries (1770)*, in *Oeuvres*, volume 3, pp. 5–73 (Gauthier-Villars, Paris), reprint of Mém. de l'Acad. Roy. des Sciences de Berlin **24**, 251–326 (1770), <http://books.google.com/books?id=YwPAAAIAAJ&pg=PA5>.
- P. S. Laplace, 1829, *Celestial Mechanics (1799)*, volume 1 (Hillard, Gray, Little, & Wilkins, Boston), translation with commentary of *Mécanique Céleste*, by N. I. Bowditch, <http://books.google.com/books?id=k-cRAAAIAAJ>.
- A. M. Legendre, 1789, *Mémoire sur les opérations trigonométriques, dont les résultats dépendent de la figure de la Terre*, Mém. de l'Acad. Roy. des Sciences de Paris, 1787, pp. 352–383, <http://books.google.com/books?id=0uIEAAAIAAJ&pg=PA352>.
- , 1806, *Analyse des triangles tracés sur la surface d'un sphéroïde*, Mém. de l'Inst. Nat. de France, 1st sem., pp. 130–161, <http://books.google.com/books?id=-d0EAAAIAAJ&pg=PA130-IA4>.
- , 1811, *Exercices de Calcul Intégral sur Divers Ordres de Transcendantes et sur les Quadratures*, volume 1 (Courcier, Paris), <http://books.google.com/books?id=riIOAAAIAAJ>.
- I. G. Letoval'tsev, 1963, *Generalization of the gnomonic projection for a spheroid and the principal geodetic problems involved in the alignment of surface routes*, Geodesy and Aerophotography, **5**, 271–274, translation of Geodeziya i Aerofotos'emka **5**, 61–68 (1963).
- J.-J. Levallois, 1970, *Géodésie Générale*, volume 2 (Eyrolles, Paris), <http://www.worldcat.org/oclc/3870605>.
- J.-J. Levallois and M. Dupuy, 1952, *Note sur le calcul des grandes géodésiques*, Technical report, IGN, Paris, <http://www.worldcat.org/oclc/31726404>.
- E. Luther, 1856, *Jacobi's Ableitung in seinem Aufsatz: "Solution nouvelle d'un problème de géodésie fondamentale" enthaltenen Formeln*, Astron. Nachr., **42**(1006), 337–358, doi:10.1002/asna.

- 18550422201, <http://adsabs.harvard.edu/abs/1856AN.....42..337J>.
 Maxima, 2009, *A computer algebra system, version 5.20.1*, <http://maxima.sf.net>.
- R. D. Miller, 1994, *Computing the area of a spherical polygon*, in P. S. Heckbert, editor, *Graphics Gems IV*, pp. 132–137 (Academic Press), <http://www.worldcat.org/oclc/29565566>.
- F. Minding, 1830, *Über die Curven des kürzesten Perimeters auf krummen Flächen*, *J. Reine Angew. Math.*, **5**, 297–304, doi:10.1515/crll.1830.5.297, <http://books.google.com/books?id=Y6wGAAAAYAAJ&pg=PA297>.
- F. W. J. Olver, D. W. Lozier, R. F. Boisvert, and C. W. Clark, editors, 2010, *NIST Handbook of Mathematical Functions* (Cambridge Univ. Press), <http://dlmf.nist.gov>.
- B. Oriani, 1806, *Elementi di trigonometria sferoidica, Pt. 1*, *Mem. dell'Ist. Naz. Ital.*, **1**(1), 118–198, <http://www.archive.org/stream/memoriadellistit11isti#page/118>.
- , 1808, *Elementi di trigonometria sferoidica, Pt. 2*, *Mem. dell'Ist. Naz. Ital.*, **2**(1), 1–58, <http://www.archive.org/stream/memoriadellistit21isti#page/1>.
- , 1810, *Elementi di trigonometria sferoidica, Pt. 3*, *Mem. dell'Ist. Naz. Ital.*, **2**(2), 1–58, <http://www.archive.org/stream/memoriadellistit22isti#page/1>.
- , 1833, *Nota aggiunta agli elementi della trigonometria sferoidica*, *Mem. dell'Imp. Reg. Ist. del Regno Lombardo-Veneto*, **4**, 325–331, <http://books.google.com/books?id=6bsAAAAAYAAJ&pg=PA325>.
- M. E. Pittman, 1986, *Precision direct and inverse solutions of the geodesic*, *Surveying and Mapping*, **46**(1), 47–54.
- L. Puissant, 1831, *Nouvel essai de trigonométrie sphéroïdique*, *Mém. de l'Acad. Roy. des Sciences de l'Inst. de France*, **10**, 457–529, <http://books.google.com/books?id=KcjOAAAAMAAJ&pg=RA2-PA457>.
- H. F. Rainsford, 1955, *Long geodesics on the ellipsoid*, *Bull. Géod.*, **37**(1), 12–22, doi:10.1007/BF02527187.
- R. H. Rapp, 1991, *Geometric geodesy, part I*, Technical report, Ohio State Univ., <http://hdl.handle.net/1811/24333>.
- , 1993, *Geometric geodesy, part II*, Technical report, Ohio State Univ., <http://hdl.handle.net/1811/24409>.
- RNAV, 2007, *Order 8260.54A, The United States Standard for Area Navigation*, U.S. Federal Aviation Administration, Washington, DC, http://www.faa.gov/documentLibrary/media/Order/8260_54A.pdf.
- T. Saito, 1970, *The computation of long geodesics on the ellipsoid by non-series expanding procedure*, *Bull. Géod.*, **98**(1), 341–373, doi:10.1007/BF02522166.
- , 1979, *The computation of long geodesics on the ellipsoid through Gaussian quadrature*, *J. Geod.*, **53**(2), 165–177, doi:10.1007/BF02521087.
- H. Schmidt, 2000, *Berechnung geodätischer Linien auf dem Rotationsellipsoid im Grenzbereich diametraler Endpunkte*, *Z. f. Vermess.*, **125**(2), 61–64, http://www.gia.rwth-aachen.de/Forschung/AngwGeodaesie/geodaetische_linie/artikel2/.
- L. E. Sjöberg, 2002, *Intersections on the sphere and ellipsoid*, *J. Geod.*, **76**(2), 115–120, doi:10.1007/s00190-001-0230-9.
- , 2006, *Determination of areas on the plane, sphere, and ellipsoid*, *Survey Review*, **38**(301), 583–593.
- J. P. Snyder, 1987, *Map projection—a working manual*, Professional Paper 1395, U.S. Geological Survey, <http://pubs.er.usgs.gov/publication/pp1395>.
- E. M. Sodano, 1958, *A rigorous non-iterative procedure for rapid inverse solution of very long geodesics*, *Bull. Géod.*, **48**(1), 13–25, doi:10.1007/BF02537675.
- TALOS, 2006, *A Manual on Technical Aspects of the United Nations Convention on the Law of the Sea, 1982*, International Hydrographic Bureau, Monaco, 4th edition, http://www.iho-ohi.net/iho_pubs/CB/S-51_Ed4-EN.pdf.
- W. M. Tobey, 1928, *Geodesy*, Technical Report 11, Geodetic Survey of Canada, Ottawa, <http://www.worldcat.org/oclc/839082>.
- I. Todhunter, 1871, *Spherical Trigonometry* (Macmillan, London), 3rd edition, <http://books.google.com/books?id=3uBHAAAAIAAJ>.
- H. Vermeille, 2002, *Direct transformation from geocentric coordinates to geodetic coordinates*, *J. Geod.*, **76**(9), 451–454, doi:10.1007/s00190-002-0273-6.
- , 2011, *An analytical method to transform geocentric into geodetic coordinates*, *J. Geod.*, **85**(2), 105–117, doi:10.1007/s00190-010-0419-x.
- T. Vincenty, 1975a, *Direct and inverse solutions of geodesics on the ellipsoid with application of nested equations*, *Survey Review*, **23**(176), 88–93, addendum: *Survey Review* **23**(180), 294 (1976), http://www.ngs.noaa.gov/PUBS_LIB/inverse.pdf.
- , 1975b, *Geodetic inverse solution between antipodal points*, unpublished report dated Aug. 28, <http://geographiclib.sf.net/geodesic-papers/vincenty75b.pdf>.
- J. Weingarten, 1863, *Über die Oberflächen für welche einer der beiden Hauptkrümmungshalbmesser eine function des anderen ist*, *J. Reine Angew. Math.*, **62**, 160–173, doi:10.1515/crll.1863.62.160, <http://books.google.com/books?id=ggRCAAAAcAAJ&pg=PA160>.
- P. Wessel and W. H. F. Smith, 2010, *Generic mapping tools, 4.5.5*, <http://gmt.soest.hawaii.edu/>.
- E. A. Williams, 2002, *Navigation on the spheroidal earth*, <http://williams.best.vwh.net/ellipsoid/ellipsoid.html>.
- R. Williams, 1997, *Gnomonic projection of the surface of an ellipsoid*, *J. Nav.*, **50**(2), 314–320, doi:10.1017/S0373463300023936.